SCIENCE CHINA
Physics, Mechanics & Astronomy

• Article •

April 2023 Vol. 66 No. 4: 240312
https://doi.org/10.1007/s11433-022-2067-x

Extension of Noether's theorem in $\mathcal{PT}$-symmetry systems and its experimental demonstration in an optical setup

Qi-Cheng Wu[1†], Jun-Long Zhao[1†], Yu-Liang Fang[1], Yu Zhang[1,2], Dong-Xu Chen[1*], Chui-Ping Yang[1,3*], and Franco Nori[4,5,6*]

[1] *Quantum Information Research Center, Shangrao Normal University, Shangrao 334001, China;*
[2] *School of Physics, Nanjing University, Nanjing 210093, China;*
[3] *Department of Physics, Hangzhou Normal University, Hangzhou 311121, China;*
[4] *Theoretical Quantum Physics Laboratory, RIKEN, Wako-shi, Saitama 351-0198, Japan;*
[5] *RIKEN Center for Quantum Computing, RIKEN, Wako-shi, Saitama 351-0198, Japan;*
[6] *Physics Department, The University of Michigan, Ann Arbor 48109-1040, USA*

Received December 14, 2022; accepted January 13, 2023; published online March 1, 2023

Noether's theorem is one of the fundamental laws in physics, relating the symmetry of a physical system to its constant of motion and conservation law. On the other hand, there exist a variety of non-Hermitian parity-time ($\mathcal{PT}$)-symmetric systems, which exhibit novel quantum properties and have attracted increasing interest. In this work, we extend Noether's theorem to a class of significant $\mathcal{PT}$-symmetry systems for which the eigenvalues of the $\mathcal{PT}$-symmetry Hamiltonian $\hat{H}_{\mathcal{PT}}$ change from purely real numbers to purely imaginary numbers, and introduce a generalized expectation value of an operator based on biorthogonal quantum mechanics. We find that the generalized expectation value of a time-independent operator is a constant of motion when the operator presents a standard symmetry in the $\mathcal{PT}$-symmetry unbroken regime, or a chiral symmetry in the $\mathcal{PT}$-symmetry broken regime. In addition, we experimentally investigate the extended Noether's theorem in $\mathcal{PT}$-symmetry single-qubit and two-qubit systems using an optical setup. Our experiment demonstrates the existence of the constant of motion and reveals how this constant of motion can be used to judge whether the $\mathcal{PT}$-symmetry of a system is broken. Furthermore, a novel phenomenon of masking quantum information is first observed in a $\mathcal{PT}$-symmetry two-qubit system. This study not only contributes to full understanding of the relation between symmetry and conservation law in $\mathcal{PT}$-symmetry physics, but also has potential applications in quantum information theory and quantum communication protocols.

Noether's theorem, $\mathcal{PT}$-symmetry systems, chiral symmetry, optical setup

PACS number(s): 03.65.Ca, 03.65.Yz, 11.30.Rd, 42.50.Xa

Citation: Q.-C. Wu, J.-L. Zhao, Y.-L. Fang, Y. Zhang, D.-X. Chen, C.-P. Yang, and F. Nori, Extension of Noether's theorem in $\mathcal{PT}$-symmetry systems and its experimental demonstration in an optical setup, Sci. China-Phys. Mech. Astron. **66**, 240312 (2023), https://doi.org/10.1007/s11433-022-2067-x

1 Introduction

The subject of finding the symmetries of dynamics is of fundamental interest and has broad applications in physics, e.g., high-energy scattering experiments, control issues in mesoscopic physics and quantum cosmology [1-6]. On the other hand, by means of symmetries, one can generally make non-trivial inferences from complex systems, such as many-body systems, dissipative systems and non-Hermitian sys-

*Corresponding authors (Dong-Xu Chen, email: chendx@sru.edu.cn; Chui-Ping Yang, email: yangcp@hznu.edu.cn; Franco Nori, email: fnori@riken.jp)
†These authors contributed equally to this work.

tems. As an important theorem which is related to symmetries, Noether's theorem [7] has important applications in quantum physics and quantum information science [8-13]. Noether's theorem states that every symmetry of dynamics implies a conservation law, and it was originally applied in Lagrangian approach in classical mechanics to uncover conserved quantities from symmetries of the Lagrangian. In many cases, the existence of these conserved quantities is very important for understanding the physical states and the properties of the systems [8, 10, 12, 13]. The theorem applies also in quantum mechanics, and the most prominent example of Noether's theorem is Ehrenfest's theorem in closed systems [9, 14]

$$\frac{\mathrm{d}}{\mathrm{d}t}\langle\hat{F}\rangle = \frac{1}{\mathrm{i}\hbar}\langle[\hat{F},\hat{H}]\rangle + \left\langle\frac{\mathrm{d}\hat{F}}{\mathrm{d}t}\right\rangle. \tag{1}$$

For an operator $\hat{F}$ without explicit time dependence, it then follows that its expectation value $\langle\hat{F}\rangle$ is a constant of motion if it commutes with the Hermitian Hamiltonian $\hat{H}$. However, Ehrenfest's theorem is not applicable for open systems [11, 14-17]. Furthermore, even in closed systems, Ehrenfest's conservation law cannot capture all features of symmetry when mixed states are considered [10].

A natural extension of Noether's theorem in non-Hermitian systems is to replace the Hermitian Hamiltonian $\hat{H}$ with a non-Hermitian Hamiltonian $\hat{H}^\dagger$, which turns eq. (1) into $\mathrm{d}\langle\hat{F}\rangle/\mathrm{d}t = \frac{1}{\mathrm{i}\hbar}\langle[\hat{F}\hat{H} - \hat{H}^\dagger\hat{F}]\rangle + \langle\mathrm{d}\hat{F}/\mathrm{d}t\rangle$ [18-21]. Up to now, based on the important intertwining relation $\hat{F}\hat{H} = \hat{H}^\dagger\hat{F}$ [19-21], several methods have been proposed to obtain conserved quantities, including spectral decomposition methods [22, 23], recursive construction of intertwining operators [24], sum-rules method [21], Stokes parametrization approach [25], and so on. Recently, the authors in ref. [26] investigated a manifestation of Noether's theorem in non-Hermitian systems, where an inner product was defined as $(\varphi,\psi) \equiv \varphi_u^{\mathrm{T}}\psi_v$ without its complex conjugation. In their framework, a generalized symmetry, which they termed pseudochirality, emerges naturally as the counterpart of the symmetry defined by the commutation relation in quantum mechanics. Some existing studies [9-26] enrich the understanding of obtaining conserved quantity beyond the Hermitian framework, whereas a full understanding of the relation between symmetry and conservation law, and practical methods for extracting expectation values in non-Hermitian systems, remain elusive. Therefore, in order to properly deal with conservation problems using Noether's theorem and explore its potential applications in non-Hermitian systems, there is an urgent need to extend Noether's theorem to non-Hermitian systems.

Over the past decades, there is considerable interest in the study of the dynamic properties of parity-time ($\mathcal{PT}$)-symmetry non-Hermitian systems [27-34]. The unique properties of $\mathcal{PT}$-symmetry systems and their applications have been investigated in various physical systems [35-44]. Moreover, many remarkable and unexpected quantum phenomena have been observed in $\mathcal{PT}$-symmetry systems, such as critical phenomena [45, 46], chiral population transfer [47, 48], information retrieval [49, 50], coherence flow [51], and topological invariants [52, 53]. A complete characterization of conservation laws in $\mathcal{PT}$-symmetry systems has been intensely explored [23, 24]. For example, based on the intertwining relation [19-21], ref. [24] has presented a complete set of conserved observables for a class of $\mathcal{PT}$-symmetry Hamiltonians in a single-photon linear optical circuit. Moreover, in the pseudo-Hermitian representation of quantum mechanics [22], ref. [54] has further implemented a model circuit of a generic anti-$\mathcal{PT}$-symmetry system. A counterintuitive energy-difference conserving dynamics has been observed [54], which is in stark contrast to the standard Hermitian dynamics keeping the system's total energy constant. However, based on biorthogonal quantum mechanics, the manifestation of Noether's theorem and a complete observation of conserved quantities in $\mathcal{PT}$-symmetry systems and their consequences are still lacking both theoretically and experimentally.

In this work, we extend Noether's theorem to a class of significant $\mathcal{PT}$-symmetry non-Hermitian systems and introduce a generalized expectation value of a time-independent operator based on biorthogonal quantum mechanics [55-58]. For the $\mathcal{PT}$-symmetry systems considered here, the eigenvalues of the $\mathcal{PT}$-symmetry Hamiltonian $\hat{H}_{\mathcal{PT}}$ change from purely real numbers to purely imaginary numbers. Such $\mathcal{PT}$-symmetry systems have been widely used to investigate the dynamics of non-Hermitian systems in the presence of balanced gain and loss [24, 26, 39, 45, 49-51]. Our work shows that the extended Noether's theorem can be used to deal with conservation law problems about pure states and mixed states. Remarkably, we find that for an operator $\hat{F}$ without explicit time dependence, its generalized expectation value is a constant of motion if $\hat{F}$ presents a standard symmetry in the $\mathcal{PT}$-symmetry unbroken regime, or a chiral symmetry in the $\mathcal{PT}$-symmetry broken regime. In addition, we experimentally investigate the extended Noether's theorem in $\mathcal{PT}$-symmetry single-qubit and two-qubit systems using an optical setup. Several novel results are found. First, our experiment demonstrates the existence of the constant of motion. Second, our experiment reveals that the constant of motion can be used to judge whether the $\mathcal{PT}$ symmetry of a system is broken. Last, our experiment reveals the phenomenon of masking quantum information [59, 60] in a $\mathcal{PT}$-symmetry two-qubit system.

2 Extension of Noether's theorem in $\mathcal{PT}$-symmetry systems

To extend Noether's theorem to $\mathcal{PT}$-symmetry systems, the biorthogonal quantum mechanics [55-58] is applied. In biorthogonal quantum mechanics, the inner product is defined as:

$$(\varphi, \psi) \equiv \langle\widehat{\varphi}|\psi\rangle = \sum_{k,l} d_k^* c_l \langle\widehat{\phi_k}|\phi_l\rangle = \sum_k d_k^* c_k, \tag{2}$$

where $|\psi\rangle = \Sigma_l c_l|\phi_l\rangle$ ($|\varphi\rangle = \Sigma_k d_k|\phi_k\rangle$) is an arbitrary pure state with its associated state $\langle\widehat{\psi}| \equiv \Sigma_l c_l^* \langle\widehat{\phi_l}|$ ($\langle\widehat{\varphi}| \equiv \Sigma_k d_k^* \langle\widehat{\phi_k}|$), and $\{\langle\widehat{\phi_{l(k)}}|\}$ and $\{|\phi_{l(k)}\rangle\}$ are left and right eigenstates of a non-Hermitian Hamiltonian (Appendixes A1 and A2).

Here, we use $\hat\rho$ ($\hat\rho_b$) to denote a density operator in standard (biorthogonal) quantum mechanics. Without loss of generality, let us consider the $\mathcal{PT}$-symmetry system to be in a mixed state $\hat\rho_b(t) = \sum_{n=1}^N p_n|\psi_n(t)\rangle\langle\widehat{\psi_n(t)}|$, p_n is the probability of the system being in a pure state $|\psi_n(t)\rangle$, with $\langle\widehat{\psi_n}(t)|\psi_n(t)\rangle = 1$. With the inner product introduced in eq. (2), a generalized expectation value $(\hat F)$ of an operator $\hat F$ can be defined (see Appendix A3)

$$\begin{aligned}(\hat F) &= \mathrm{tr}[\hat\rho_b(t)\hat F] = \sum_l \langle\widehat{\phi_l}|\hat\rho_b(t)\hat F|\phi_l\rangle \\ &= \sum_n p_n \langle\widehat{\psi_n(t)}|\hat F|\psi_n(t)\rangle,\end{aligned} \tag{3}$$

where $\langle\widehat{\psi_n(t)}|\hat F|\psi_n(t)\rangle$ is the generalized expectation value $(\hat F)$ of the operator $\hat F$ for an arbitrary pure state $|\psi_n(t)\rangle$. Eq. (3) provides a natural generalization of expectation value of an operator $\hat F$ for an arbitrary quantum state, either a mixed state or a pure state.

As one of the main contributions of this work, we find that the temporal evolution of the expectation value $(\hat F)$ of the operator $\hat F$ follows two different forms (see Appendix A3 for the detailed derivation):

$$\frac{\mathrm{d}}{\mathrm{d}t}(\hat F) = \sum_n p_n \left[\frac{1}{\mathrm{i}\hbar}([\hat F, \hat H_{\mathcal{PT}}])_n + \left(\frac{\mathrm{d}\hat F}{\mathrm{d}t}\right)_n\right], \tag{4}$$

$$\frac{\mathrm{d}}{\mathrm{d}t}(\hat F) = \sum_n p_n \left[\frac{1}{\mathrm{i}\hbar}(\{\hat F, \hat H_{\mathcal{PT}}\})_n + \left(\frac{\mathrm{d}\hat F}{\mathrm{d}t}\right)_n\right], \tag{5}$$

where $(\cdot)_n = \langle\widehat{\psi_n(t)}| \cdot |\psi_n(t)\rangle$. Eq. (4) corresponds to the case when the system works in the $\mathcal{PT}$-symmetry unbroken regime, while eq. (5) corresponds to the case when the system works in the $\mathcal{PT}$-symmetry broken regime. From eq. (4), one can see that the expectation value $(\hat F)$ is a constant of motion if the Hamiltonian $\hat H_{\mathcal{PT}}$ and the time-independent operator $\hat F$ satisfy the commutation relation $[\hat F, \hat H_{\mathcal{PT}}] = 0$, i.e., the operator $\hat F$ presents a standard symmetry in the $\mathcal{PT}$-symmetry unbroken regime [1]. On the other hand, eq. (5) implies that the expectation value $(\hat F)$ is also a constant of motion if $\hat H_{\mathcal{PT}}$ and $\hat F$ satisfy the anti-commutation relation $\{\hat F, \hat H_{\mathcal{PT}}\} = 0$, i.e., $\hat F$ presents a chiral symmetry in the $\mathcal{PT}$-symmetry broken regime [2].

To understand the above results intuitively, let us consider a $\mathcal{PT}$-symmetry single-qubit system where the eigenvalues of the Hamiltonian change from real (in the $\mathcal{PT}$-symmetry unbroken regime), to purely imaginary (in the $\mathcal{PT}$-symmetry broken regime). The Hamiltonian for this system is given by (hereafter, we assume $\hbar = 1$)

$$\hat H_{\mathcal{PT}} = s\hat\sigma_x + \mathrm{i}\gamma\hat\sigma_z = \begin{pmatrix} \mathrm{i}\gamma & s \\ s & -\mathrm{i}\gamma \end{pmatrix}, \tag{6}$$

where $\mathrm{i}\gamma\hat\sigma_z$ is the non-Hermitian part of the Hamiltonian governing gain and loss [27, 61]. The parameter $s > 0$ is an energy scale, $a = \gamma/s > 0$ is a coefficient representing the degree of non-Hermiticity, $\hat\sigma_x$ and $\hat\sigma_z$ are the standard Pauli operators. The eigenvalues of $\hat H_{\mathcal{PT}}$ are given by $E_1 = s\sqrt{1-a^2}$ and $E_2 = -s\sqrt{1-a^2}$, which are real numbers for $0 < a < 1$ (the $\mathcal{PT}$-symmetry unbroken regime), while purely imaginary numbers for $a > 1$ (the $\mathcal{PT}$-symmetry broken regime). The right eigenvectors of $\hat H_{\mathcal{PT}}$ are $|\phi_1\rangle = f_1\times(A_1|0\rangle+|1\rangle)$ and $|\phi_2\rangle = f_2\times(A_2|0\rangle+|1\rangle)$, while the left eigenvectors of $\hat H_{\mathcal{PT}}$ are $\langle\widehat{\phi_1}| = f_3^*\times(-A_2^*\langle 0| + \langle 1|)$ and $\langle\widehat{\phi_2}| = f_4^*\times(-A_1^*\langle 0| + \langle 1|)$ (Appendix A2). Here, $A_1 = \mathrm{i}a + \sqrt{1-a^2}$, $A_2 = \mathrm{i}a - \sqrt{1-a^2}$, and f_1, f_2, f_3, f_4 satisfy $f_1\cdot f_3^*\times(1-A_2^*A_1) = f_2\cdot f_4^*\times(1-A_1^*A_2) = 1$ to satisfy the biorthogonality and closure relations.

The Hamiltonian (6) can be considered as a deformed Pauli operator, $\hat H_{\mathcal{PT}} = E_1|\phi_1\rangle\langle\widehat{\phi_1}| - E_1|\phi_2\rangle\langle\widehat{\phi_2}|$, in view of the biorthogonal partners $\{|\phi_1\rangle, |\phi_2\rangle\}$ and $\{\langle\widehat{\phi_1}|, \langle\widehat{\phi_2}|\}$ (Appendixes A1 and A2). If a time-independent operator $\hat F$ can be expressed in the form:

$$\hat F = c_1|\phi_1\rangle\langle\widehat{\phi_1}| + c_2|\phi_2\rangle\langle\widehat{\phi_2}|, \tag{7}$$

where c_1 and c_2 are arbitrary nonzero coefficients, one can easily verify $[\hat F, \hat H_{\mathcal{PT}}] = 0$. Thus, according to eq. (4), the expectation value $(\hat F)$ is a constant of motion in the $\mathcal{PT}$-symmetry unbroken regime. On the other hand, if a time-independent operator $\hat F$ can be expressed in the form:

$$\hat F = \tilde c_1(|\phi_1\rangle\langle\widehat{\phi_2}| - |\phi_2\rangle\langle\widehat{\phi_1}|), \tag{8}$$

where $\tilde c_1$ is an arbitrary nonzero coefficient, one can obtain $\{\hat F, \hat H_{\mathcal{PT}}\} = 0$. In this case, according to eq. (5), the expectation value $(\hat F)$ is a constant of motion in the $\mathcal{PT}$-symmetry broken regime. From an experimental point of view, in order to keep the expectation value $(\hat F)$ as a real number, the chosen operator $\hat F$ should be Hermitian in biorthogonal quantum mechanics (see Appendix A4). Therefore, in the subsequent discussion, the coefficients c_1 and c_2 in eq. (7) are chosen as real numbers, and the coefficient $\tilde c_1$ in eq. (8) is chosen as a purely imaginary number.

3 Experimental setup

3.1 Single-qubit case

The apparatus for the initial state preparation in a single-photon system is illustrated in Figure 1(a), where a single photon acts as the qubit. A photon pair is generated through a type-I phase-matched spontaneous parametric down-conversion process. The idler photon is detected by a single photon detector as a trigger. The qubit is encoded by the polarization of the heralded single photon, with $|0\rangle = |H\rangle$ and $|1\rangle = |V\rangle$. The initial state is prepared by a polarization beam splitter (PBS) and a half-wave plate (HWP). Then the photon is injected into a time-evolution toolbox, which outputs the desired time-evolved state. In our experiment, the time-evolved state is accessed by enforcing the time-evolution operator $\hat{U}_{\mathcal{PT}}(t)$=$\exp(-\mathrm{i}\hat{H}_{\mathcal{PT}}t)$ at any given time on the initial state. Here, the Hamiltonian $\hat{H}_{\mathcal{PT}}$ is the one given by eq. (6). As depicted in Figure 1(c), the time-evolution toolbox implements the time-evolution operator $\hat{U}_{\mathcal{PT}}(t)$ by decomposing it into basic operations (see Appendix A5)

$$\begin{aligned}\hat{U}_{\mathcal{PT}}(t) =&\hat{R}_{\mathrm{QWP}}(\pi/4)\hat{R}_{\mathrm{HWP}}(\theta_3)\hat{R}_{\mathrm{QWP}}(\theta_2)\hat{L}(\xi_1,\ \xi_2)\\ &\times \hat{R}_{\mathrm{HWP}}(0)\hat{R}_{\mathrm{HWP}}(\theta_1)\hat{R}_{\mathrm{QWP}}(0),\end{aligned} \tag{9}$$

where the loss-dependent operator

$$\hat{L}(\xi_1,\ \xi_2) = \begin{pmatrix} 0 & \sin 2\xi_1 \\ \sin 2\xi_2 & 0 \end{pmatrix} \tag{10}$$

is realized by a combination of two beam displacers (BDs) and two HWPs with setting angles ξ_1 and ξ_2 (ξ_2 is fixed with $\pi/4$ in our experiment). Moreover, $\hat{R}_{\mathrm{HWP}}$ and $\hat{R}_{\mathrm{QWP}}$ are the rotation operators of the HWP and quarter-wave plate (QWP), respectively.

The time-evolved states in the $\mathcal{PT}$-symmetry single-qubit system are given by [49, 62, 63]

$$\hat{\rho}^E(t) = \frac{\hat{U}_{\mathcal{PT}}(t)\hat{\rho}(0)\hat{U}^{\dagger}_{\mathcal{PT}}(t)}{\mathrm{Tr}\left[\hat{U}_{\mathcal{PT}}(t)\hat{\rho}(0)\hat{U}^{\dagger}_{\mathcal{PT}}(t)\right]}, \tag{11}$$

where $\hat{\rho}(0)$ is the initial density matrix and $\hat{\rho}^E(t)$ is the experimental density matrix at any given time t in standard quantum mechanics. The density matrix $\rho^E(t)$ can be constructed via quantum state tomography [64, 65]. For the single-qubit system, we project the photon onto 4 bases $\{|H\rangle, |V\rangle, |R\rangle = (|H\rangle - \mathrm{i}|V\rangle)/\sqrt{2}, |D\rangle = (|H\rangle + |V\rangle)/\sqrt{2}\}$. In addition, we note that the density matrix in biorthogonal quantum mechanics can be reversely extracted from the density matrix in standard quantum mechanics $\hat{\rho}^E(t)$ (Appendix A6). On the other hand, the density matrix $\hat{\rho}_b(t)$ in biorthogonal quantum mechanics can be obtained according to the following relationships (Appendix A7):

$$\hat{\rho}_b(t) = \hat{U}_{\mathcal{PT}}(t)\hat{\rho}_b(0)\hat{U}'_{\mathcal{PT}}(t), \tag{12}$$

$$\hat{\rho}_b(t) = \hat{U}_{\mathcal{PT}}(t)\hat{\rho}_b(0)\hat{U}_{\mathcal{PT}}(t), \tag{13}$$

where $\hat{U}_{\mathcal{PT}}(t)$=$\exp(-\mathrm{i}\hat{H}_{\mathcal{PT}}t)$ and $\hat{U}'_{\mathcal{PT}}(t)$=$\exp(\mathrm{i}\hat{H}_{\mathcal{PT}}t)$ are time-evolution operators, and $\hat{\rho}_b(0)$ is the initial density matrix in biorthogonal quantum mechanics. Eqs. (12) and (13)

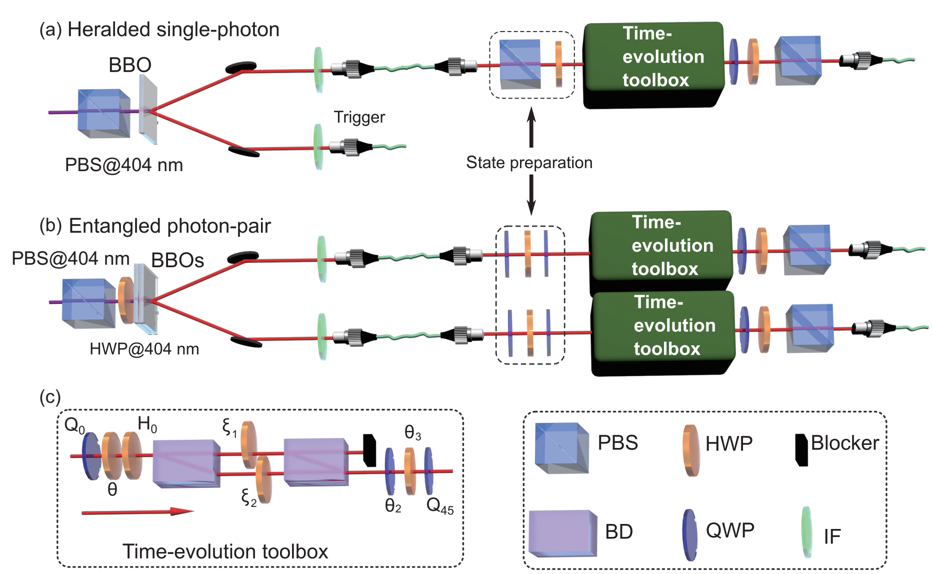

Figure 1 (Color online) Experimental setup. (a) Overview of the apparatus for the initial state preparation in a single-photon system. For details, please refer to the text. (b) Overview of the apparatus for the initial state preparation in a two-photon system. For details, please refer to the text. (c) Implementation of the time-evolution toolbox. Q_0 (H_0) represents a QWP (HWP) with fixed orientation 0°, while Q_{45} represents an QWP with fixed orientation $\pi/4$. See text for details. PBS, polarization beam splitter; HWP, half-wave plate; QWP, quarter-wave plate; BD, beam displacer; IF, interference filter; BBO, β-barium-borate crystal.

correspond to the cases when the system evolves in the $\mathcal{PT}$-symmetry unbroken regime and $\mathcal{PT}$-symmetry broken regime, respectively.

3.2 Two-qubit case

The apparatus for the initial state preparation in a two-photon system is illustrated in Figure 1(b). The entangled states in the experiment are generated through a type-II phase-matched spontaneous parametric down-conversion. Then two combinations of HWPs and QWPs (i.e., the upper and lower parts in the dashed box) operating on each photon, eliminate the influence caused by the fibres, therefore preparing the initial state. Then each photon is injected into a $\mathcal{PT}$-symmetry time evolution toolbox. The dynamical evolution of quantum states in this case is similarly given by eq. (11), where the time-evolution nonunitary operator is now given by $\hat{U}_{\mathcal{PT}}(t) = \hat{U}_{\mathcal{PT},1}(t) \otimes \hat{U}_{\mathcal{PT},2}(t)$. Here, $\hat{U}_{\mathcal{PT},j}(t) = \exp(-\mathrm{i}\hat{H}_{\mathcal{PT},j}t)$ $(j = 1, 2)$ is the time-evolution nonunitary operator of qubit j in the two-qubit system. Experimentally, we reconstruct the density matrix $\hat{\rho}^E(t)$ at any given time t via quantum state tomography after each of the two photons passes through the time-evolution toolbox. Essentially, we project the two-qubit state onto 16 basis states through a combination of QWP, HWP and PBS, and then perform a maximum-likelihood estimation of the density matrix [64, 65].

3.3 Device parameters

For the single-qubit case, the photon pair is generated through a type-I phase-matched spontaneous parametric down-conversion process by pumping a nonlinear β-barium-borate (BBO) crystal with a 404 nm pump laser, where the BBO crystal is 3 mm thick. The power of the pump laser is 130 mW. The bandwidth of the interference filter (IF) is 10 nm. This yields a maximum count of 60000 per second. The quantum state is measured by performing standard state tomography, i.e., projecting the state onto 4 bases $\{|H\rangle, |V\rangle, |R\rangle = (|H\rangle - \mathrm{i}|V\rangle)/\sqrt{2}, |D\rangle = (|H\rangle + |V\rangle)/\sqrt{2}\}$, and the corresponding angles of QWP-HWP are (0°, 0°), (0°, 45°), (45°, 22.5°), (0°, 22.5°), and (45°, 0°), respectively.

For the two-qubit case, the entangled states in the experiment are generated through a type-II phase-matched spontaneous parametric down-conversion, by pumping two BBO crystals with a 404 nm pump laser, where each BBO crystal is 0.4 mm thick and the optical axes are perpendicular to each other. The measurement of the photon source yields a maximum of 10000 photon counts over 1.5 s after the 10 nm IF. Here, the quantum state is measured by performing standard state tomography, i.e., projecting the state onto 16 bases $\{|HH\rangle, |HV\rangle, |VV\rangle, |VH\rangle, |RH\rangle, |RV\rangle, |DV\rangle, |DH\rangle, |DR\rangle, |DD\rangle, |RD\rangle, |HD\rangle, |VD\rangle, |VL\rangle, |HL\rangle, |RL\rangle\}$, where $|D\rangle = (|H\rangle + |V\rangle)/\sqrt{2}$, $|R\rangle = (|H\rangle - \mathrm{i}|V\rangle)/\sqrt{2}$, and $|L\rangle = (|H\rangle + \mathrm{i}|V\rangle)/\sqrt{2}$.

4 Experimental and theoretical results

4.1 Expectation values of operators in a $\mathcal{PT}$-symmetry single-qubit system

As two results derived from Noether's theorem, eqs. (7) and (8) tell us that the expectation value (F) is a constant of motion if

$$\hat{F} = \widetilde{\sigma}_z = |\phi_1\rangle\langle\widehat{\phi_1}| - |\phi_2\rangle\langle\widehat{\phi_2}|, \quad (c_1 = -c_2 = 1) \tag{14}$$

and

$$\hat{F} = \widetilde{\sigma}_y = -\mathrm{i}|\phi_1\rangle\langle\widehat{\phi_2}| + \mathrm{i}|\phi_2\rangle\langle\widehat{\phi_1}|), \quad (\tilde{c}_1 = -\mathrm{i}) \tag{15}$$

for the $\mathcal{PT}$-symmetry unbroken and broken cases, respectively. We experimentally confirm this prediction in a $\mathcal{PT}$-symmetry single-qubit system. As shown in Figure 2(a), in the $\mathcal{PT}$-symmetry unbroken regime, $(\widetilde{\sigma}_z)$ is a constant of motion, whereas $(\widetilde{\sigma}_y)$ changes over time. Interestingly, in

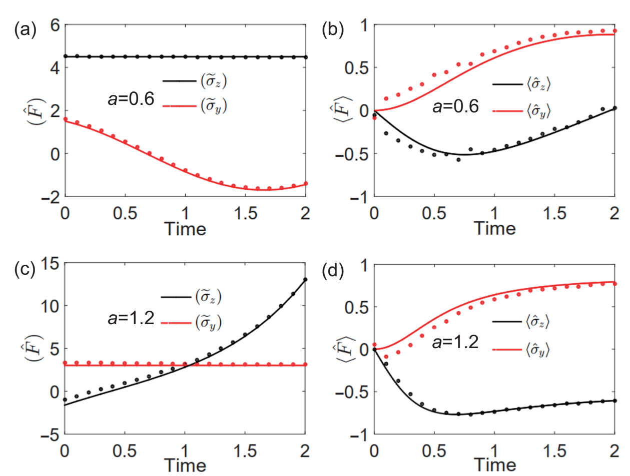

Figure 2 (Color online) The temporal evolutions of expectation values $(\hat{F})$ and $\langle\hat{F}\rangle$ in the $\mathcal{PT}$-symmetry single-photon system. For (a) and (b) the system works in the $\mathcal{PT}$-symmetry unbroken regime ($a = 0.6$), while for (c) and (d) the system works in the $\mathcal{PT}$ symmetry broken regime ($a = 1.2$). For (a) and (c), the observable operators $\hat{F}$ are chosen as deformed Pauli operators $\widetilde{\sigma}_z = |\phi_1\rangle\langle\widehat{\phi_1}| - |\phi_2\rangle\langle\widehat{\phi_1}|$ and $\widetilde{\sigma}_y = -\mathrm{i}|\phi_1\rangle\langle\widehat{\phi_2}| + \mathrm{i}|\phi_2\rangle\langle\widehat{\phi_1}|$ in biorthogonal quantum mechanics. The expectation value $(\hat{F})$ is based on $(\hat{F}) = \langle\widehat{\psi(t)}|\hat{F}|\psi(t)\rangle$. For (b) and (d), the observable operators are chosen as standard Pauli operators $\hat{\sigma}_z$ and $\hat{\sigma}_y$, and the expectation value $\langle\hat{F}\rangle$ is based on $\langle\hat{F}\rangle = \langle\psi(t)|\hat{F}|\psi(t)\rangle$. The initial state is $(|0\rangle + |1\rangle)/\sqrt{2}$, and we have set $f_1 = f_2 = 1/\sqrt{2}$ and $s = 1$. All curves show the theoretical results while dots are the experimental data.

contrast to Figure 2(a), Figure 2(c) shows that in the $\mathcal{PT}$-symmetry broken regime, $(\widetilde{\sigma}_y)$ is a constant of motion, while $(\widetilde{\sigma}_z)$ changes over time. The experimental results here agree well with the theoretical simulation results. As a contrast, we also measure the expectation values of $\hat{\sigma}_z$ and $\hat{\sigma}_y$ in standard quantum mechanics, shown in Figure 2(b) and (d). One can see from Figures 2(b) and (d) that both $\langle\hat{\sigma}_z\rangle$ and $\langle\hat{\sigma}_y\rangle$ change over time in the $\mathcal{PT}$-symmetry unbroken or broken regime, i.e., one cannot obtain a constant of motion. Hence, according to the temporal evolution of expectation values of $(\widetilde{\sigma}_z)$ and $(\widetilde{\sigma}_y)$, one can judge whether the system works in the $\mathcal{PT}$-symmetry unbroken or broken regime.

On the other hand, since our experimental apparatus is quite general and capable of implementing a broad class of nonunitary operators, we are able to investigate the role of non-Hermiticities and the effects of initial states on the temporal evolution of expectation values. It can be clearly seen from Figure 3(a) and (b) that with different initial states, $(\widetilde{\sigma}_z)$ is always a constant in the $\mathcal{PT}$-symmetry unbroken regime even though the initial state is a mixed state. However, the expectation value $(\widetilde{\sigma}_z)$ is dependent on the initial states. Comparing Figure 3(a) with Figure 3(b), one can see that the expectation value $(\widetilde{\sigma}_z)$ gradually increases when the parameter a (representing the degree of non-Hermiticity) increases. Similarly, Figure 3(c) and (d) show that in $\mathcal{PT}$-symmetry broken regime, $(\widetilde{\sigma}_y)$ is always a constant for different initial states even though the initial state is a mixed state, and the expectation value $(\widetilde{\sigma}_y)$ gradually decreases when the parameter a increases.

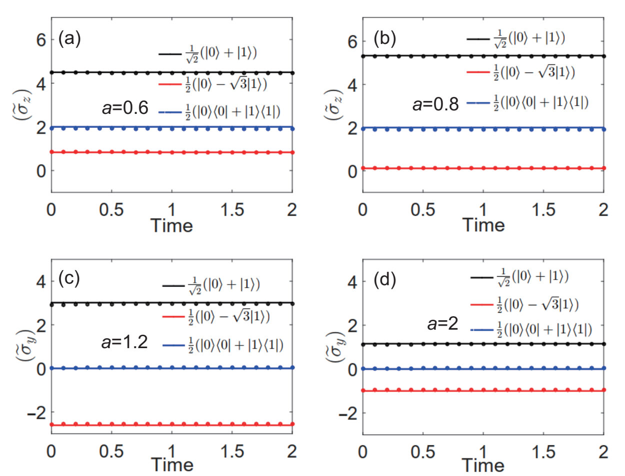

Figure 3 (Color online) The temporal evolutions of expectation values $(\widetilde{\sigma}_z)$ and $(\widetilde{\sigma}_y)$ in the $\mathcal{PT}$-symmetry single-photon system under different non-Hermiticities. The non-Hermiticities in (a)-(d) are chosen as a = 0.6, 0.8, 1.2, and 2, respectively. The initial states are chosen as two pure states $\frac{1}{\sqrt{2}}(|0\rangle + |1\rangle)$, $\frac{1}{2}(|0\rangle - \sqrt{3}|1\rangle)$ and a mixed state $\frac{1}{2}(|0\rangle\langle 0| + |1\rangle\langle 1|)$. We have set $f_1 = f_2 = 1/\sqrt{2}$ and $s = 1$. All curves show the theoretical results while dots are the experimental data.

4.2 Expectation values of operators in a $\mathcal{PT}$-symmetry two-qubit system

We further study the $\mathcal{PT}$ evolution of a two-qubit system using the optical setup shown in Figure 1(b). The Hamiltonian of the two-qubit system is described by $\hat{H}=\hat{H}_{\mathcal{PT},1}+\hat{H}_{\mathcal{PT},2}=s(\hat{S}_x+\mathrm{i}a\hat{S}_z)$, with $\hat{H}_{\mathcal{PT},j}=s(\hat{\sigma}_{x,j}+\mathrm{i}a\hat{\sigma}_{z,j})$, $\hat{S}_x=\hat{\sigma}_{x,1}+\hat{\sigma}_{x,2}$, and $\hat{S}_z=\hat{\sigma}_{z,1}+\hat{\sigma}_{z,2}$. Here, $\hat{\sigma}_{x,j}$ and $\hat{\sigma}_{z,j}$ are the standard Pauli operators for the photonic qubit j ($j = 1, 2$). The parameter s is still the energy scale. For different initial states, the temporal evolutions of expectation values in the two-qubit system are plotted in Figure 4. The observable operators in Figure 4(a) and (c) are chosen as $\widetilde{S}_y=\widetilde{\sigma}_{y,1}+\widetilde{\sigma}_{y,2}$ and $\widetilde{S}_z=\widetilde{\sigma}_{z,1}+\widetilde{\sigma}_{z,2}$, respectively. Here, $\widetilde{\sigma}_{y,j}$ and $\widetilde{\sigma}_{z,j}$ are deformed Pauli operators for the qubit j ($j = 1, 2$) in biorthogonal quantum mechanics. One can verify $\{\widetilde{S}_y, \hat{H}\} = 0$ and $[\widetilde{S}_z, \hat{H}] = 0$. As expected, Figure 4(a) and (c) show that $(\widetilde{S}_y)$ remains unchanged, whereas $(\widetilde{S}_z)$ changes quickly in the $\mathcal{PT}$-symmetry broken regime ($a = 1.2$). Remarkably, it is worth noting that the expectation value $(\widetilde{S}_y)$ is zero, which is independent of the initial states. Taking an information-theoretic perspective on this phenomenon, one can thus conclude that the information of the initial states is masked when measuring the expectation value $(\widetilde{S}_y)$, while the information of the initial states can be disclosed by measuring the expectation value $(\widetilde{S}_z)$. In addition, Figure 4(b) and (d) show that both $\langle\hat{S}_z\rangle$ and $\langle\hat{S}_y\rangle$ depend on the initial states and change over time, i.e.,

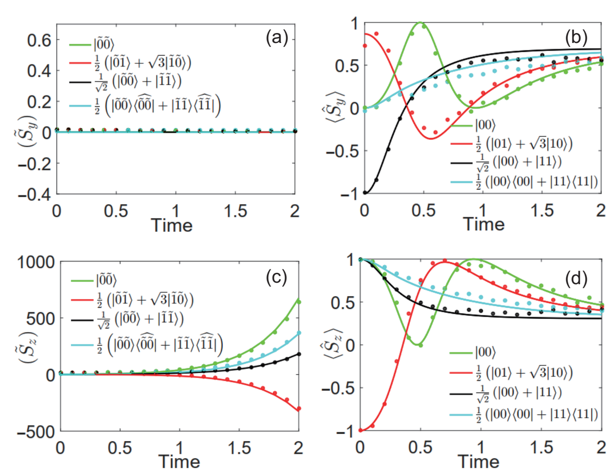

Figure 4 (Color online) The temporal evolutions of expectation values in the $\mathcal{PT}$-symmetry two-qubit system with different initial states in the $\mathcal{PT}$-symmetry broken regime ($a = 1.2$). The observable operators in (a) and (b) are chosen as $\widetilde{S}_y = \widetilde{\sigma}_{y,1} + \widetilde{\sigma}_{y,2}$, and $\hat{S}_y = \hat{\sigma}_{y,1} + \hat{\sigma}_{y,2}$, respectively; while the observable operators in (c) and (d) are chosen as $\widetilde{S}_z = \widetilde{\sigma}_{z,1} + \widetilde{\sigma}_{z,2}$, and $\hat{S}_z = \hat{\sigma}_{z,1} + \hat{\sigma}_{z,2}$, respectively. Here, $\hat{\sigma}_{x,j}$ and $\hat{\sigma}_{z,j}$ ($\widetilde{\sigma}_{x,j}$ and $\widetilde{\sigma}_{z,j}$) are the standard (deformed) Pauli operators for the qubit j ($j = 1, 2$) in standard (biorthogonal) quantum mechanics. $|\widetilde{0}\rangle \equiv |\phi_1\rangle$, $|\widetilde{1}\rangle \equiv |\phi_2\rangle$, $\langle\widetilde{\widetilde{0}}| = \langle\widehat{\phi_1}|$, $\langle\widetilde{\widetilde{1}}| = \langle\widehat{\phi_2}|$, and we set $f_1 = f_2 = 1/\sqrt{2}$ and $s = 1$. All curves show the theoretical results while dots are the experimental data.

the phenomenon of masking quantum information does not exist in standard quantum mechanics. Hence, the masking of quantum information is a unique phenomenon in biorthogonal quantum mechanics.

5 Conclusion

We have extended Noether's theorem to a class of significant $\mathcal{PT}$-symmetry non-Hermitian systems and introduced a generalized expectation value of a time-independent operator based on biorthogonal quantum mechanics. We have demonstrated that in the $\mathcal{PT}$-symmetry unbroken regime, the generalized expectation value of a time-independent operator is a constant of motion, if the time-independent operator and the non-Hermitian Hamiltonian satisfy the commutation relation, i.e., the operator presents a standard symmetry. Moreover, even in the $\mathcal{PT}$-symmetry broken regime, the expectation value of a time-independent operator is still a constant of motion provided the operator and the non-Hermitian Hamiltonian satisfy the anti-commutation relation, i.e., the operator presents a chiral symmetry. Furthermore, we have experimentally confirmed our predictions in $\mathcal{PT}$-symmetry single-qubit and two-qubit systems by using an optical setup. Our experiment has demonstrated the existence of the predicted constant of motion. Meanwhile, a novel phenomenon of masking quantum information is first observed in a $\mathcal{PT}$-symmetry two-qubit system. The extended Noether's theorem not only contributes to a full understanding of the relation between symmetry and conservation law in $\mathcal{PT}$-symmetry physics, but also has potential applications in quantum information theory and quantum communication protocols.

The present work has some elements in common with previous works on obtaining conserved quantity in non-Hermitian systems, especially the idea of using pseudo-Hermiticity (equivalently, the intertwining relation) [19-23]. Therefore, we here address the difference between our work and previous works. As shown in refs. [19,20], every Hamiltonian with a real spectrum is pseudo-Hermitian, and all the $\mathcal{PT}$-symmetry non-Hermitian Hamiltonians belong to the so-called pseudo-Hermitian Hamiltonians. In the pseudo-Hermitian representation of quantum mechanics, the expectation value $\langle\hat{F}\rangle$ of a time-independent operator $\hat{F}$ is a conserved quantity provided the intertwining relation, $\hat{F}\hat{H} = \hat{H}^{\dagger}\hat{F}$, is satisfied. In principle, a complete set of conserved observables can be obtained by numerically solving a set of N^2-dimensional linear intertwining relation [21-25]. However, a common problem, which one may encounter via pseudo-Hermiticity (intertwining relation), is how to connect the conserved quantities with the symmetries of dynamics. Compared with previous studies [19-25], the main difference of our work is that by introducing a generalized expectation value of an operator based on biorthogonal quantum mechanics, we connect two important symmetries with conserved operators in the $\mathcal{PT}$-symmetry unbroken and broken regimes, respectively. We remark that the proposed standard symmetry $\hat{F}\hat{H} = \hat{H}\hat{F}$ and the chiral symmetry $\hat{F}\hat{H} = -\hat{H}\hat{F}$ are essentially different from the intertwining relation $\hat{F}\hat{H} = \hat{H}^{\dagger}\hat{F}$, because of $\hat{H} \neq \hat{H}^{\dagger}$ and $\hat{H} \neq -\hat{H}^{\dagger}$ in $\mathcal{PT}$-symmetry systems.

We note that the extended Noether's theorem is always valid for such $\mathcal{PT}$-symmetry systems provided the eigenvalues of $\hat{H}_{\mathcal{PT}}$ change from purely real numbers to purely imaginary numbers; or equivalently, $\hat{H}_{\mathcal{PT}}$ exhibits an exceptional point of the order of the system's dimension. As an example, consider a 3-dimensional $\mathcal{PT}$-symmetry system [23], for which the Hamiltonian reads $H_{\mathcal{PT}} = sJ_x + \mathrm{i}\gamma J_z$, where J_x and J_z are the 3-dimensional angular momentum operators. Such a $\mathcal{PT}$-symmetry Hamiltonian has a third-order exceptional point at $\gamma = s$ and its spectrum also changes from real to purely imaginary [23]. Then, based on the extended Noether's theorem, one can quickly find its conserved quantities in the $\mathcal{PT}$-symmetry unbroken and broken regimes, respectively.

For any quantum system, whose Hamiltonian can be simplified to the form in eq. (6), the extended Noether's theorem presented in this work can be implemented straightforwardly. Note that for the simplified Hamiltonian, arbitrary dressed states can be chosen as basis states as long as the dressed states satisfy the biorthogonality and closure relations. This might lead to a useful step toward realizing fast symmetry discrimination and conserved quantity acquisition for multi-qubit $\mathcal{PT}$-symmetry systems. Moreover, in above discussion, we focus on the case of an operator $\hat{F}$ without explicit time dependence. However, the derived eqs. (4) and (5) also work well in a general case, i.e., the operator $\hat{F}(t)$ is time-dependent. Then, one may obtain constant of motion for a time-dependent operator in a time-dependent $\mathcal{PT}$-symmetry system, which may be interesting and attractive. Furthermore, in some sense, the $\mathcal{PT}$-symmetry Hamiltonian in eq. (6) has parallels with non-Hermitian topological phases [6, 36] and the extended classification of topological classes [3, 5]. The discovery of the relation between conserved quantities and non-Hermitian topological invariants [52, 53] is also interesting and attractive, which is a fascinating field where further extension of this work may be explored.

This work was supported by the National Natural Science Foundation of China (Grant Nos. 12264040, 12204311, 11804228, 11865013, and U21A20436), the Jiangxi Natural Science Foundation (Grant

Nos. 20212BAB211018, 20192ACBL20051), the Project of Jiangxi Province Higher Educational Science and Technology Program (Grant Nos. GJJ190891, and GJJ211735), and the Key-Area Research and Development Program of Guangdong Province (Grant No. 2018B03-0326001). Franco Nori is supported in part by the Nippon Telegraph and Telephone (NTT) Corporation Research, the Japan Science and Technology (JST) Agency [via the Quantum Leap Flagship Program (Q-LEAP), and Moonshot R&D Grant Number JPMJMS2061], the Japan Society for the Promotion of Science (JSPS) [via the Grants-in-Aid for Scientific Research (KAKENHI) Grant No. JP20H00134], the Army Research Office (ARO) (Grant No. W911NF-18-1-0358), the Asian Office of Aerospace Research and Development (AOARD) (Grant No. FA2386-20-1-4069), and the Foundational Questions Institute Fund (FQXi) (Grant No. FQXi-IAF19-06).

1 A. Altland, and M. R. Zirnbauer, Phys. Rev. B **55**, 1142 (1997), arXiv: cond-mat/9602137.
2 S. Malzard, C. Poli, and H. Schomerus, Phys. Rev. Lett. **115**, 200402 (2015), arXiv: 1508.03985.
3 Z. Gong, Y. Ashida, K. Kawabata, K. Takasan, S. Higashikawa, and M. Ueda, Phys. Rev. X **8**, 031079 (2018), arXiv: 1802.07964.
4 K. Kawabata, K. Shiozaki, M. Ueda, and M. Sato, Phys. Rev. X **9**, 041015 (2019), arXiv: 1812.09133.
5 K. Y. Bliokh, J. Dressel, and F. Nori, New J. Phys. **16**, 093037 (2014), arXiv: 1404.5486.
6 M. Li, X. Ni, M. Weiner, A. Alù, and A. B. Khanikaev, Phys. Rev. B **100**, 045423 (2019), arXiv: 1807.00913.
7 E. Noether, Transp. Theor. Statist. Phys. **1**, 186 (1971), arXiv: physics/0503066.
8 N. Ma, Y. Z. You, and Z. Y. Meng, Phys. Rev. Lett. **122**, 175701 (2019), arXiv: 1811.08823.
9 R. Shankar, *Principles of Quantum Mechanics*, 2nd ed. (Springer, New York, 1994).
10 I. Marvian, and R. W. Spekkens, Nat. Commun. **5**, 3821 (2014), arXiv: 1404.3236.
11 P. M. Zhang, M. Elbistan, P. A. Horvathy, and P. Kosiński, Eur. Phys. J. Plus **135**, 223 (2020), arXiv: 1903.05070.
12 K. Y. Bliokh, A. Y. Bekshaev, and F. Nori, New J. Phys. **15**, 033026 (2013), arXiv: 1208.4523.
13 L. Burns, K. Y. Bliokh, F. Nori, and J. Dressel, New J. Phys. **22**, 053050 (2020), arXiv: 1912.10522.
14 J. J. García-Ripoll, V. M. Pérez-García, and V. Vekslerchik, Phys. Rev. E **64**, 056602 (2001), arXiv: cond-mat/0106487.
15 Q. C. Wu, Y. H. Zhou, B. L. Ye, T. Liu, and C. P. Yang, New J. Phys. **23**, 113005 (2021).
16 D. Li, and C. Zheng, Entropy **24**, 1563 (2022).
17 X. E. Gao, D. L. Li, Z. H. Liu, and C. Zheng, Acta Phys. Sin. **71**, 240303 (2022).
18 H. Ramezani, T. Kottos, R. El-Ganainy, and D. N. Christodoulides, Phys. Rev. A **82**, 043803 (2010), arXiv: 1005.5189.
19 A. Mostafazadeh, J. Math. Phys. **43**, 205 (2002), arXiv: math-ph/0107001.
20 A. Mostafazadeh, J. Phys. A-Math. Gen. **36**, 7081 (2003), arXiv: quant-ph/0304080.
21 M. V. Berry, J. Phys. A-Math. Theor. **41**, 244007 (2008).
22 A. Mostafazadeh, Int. J. Geom. Methods Mod. Phys. **07**, 1191 (2010), arXiv: 0810.5643.
23 F. Ruzicka, K. S. Agarwal, and Y. N. Joglekar, J. Phys.-Conf. Ser. **2038**, 012021 (2021).
24 Z. Bian, L. Xiao, K. Wang, X. Zhan, F. A. Onanga, F. Ruzicka, W. Yi, Y. N. Joglekar, and P. Xue, Phys. Rev. Res. **2**, 022039 (2020), arXiv: 1903.09806.
25 M. H. Teimourpour, R. El-Ganainy, A. Eisfeld, A. Szameit, and D. N. Christodoulides, Phys. Rev. A **90**, 053817 (2014), arXiv: 1408.1561.
26 J. D. H. Rivero, and L. Ge, Phys. Rev. Lett. **125**, 083902 (2020), arXiv: 2101.09239.
27 C. M. Bender, and S. Boettcher, Phys. Rev. Lett. **80**, 5243 (1998), arXiv: physics/9712001.
28 L. Ge, Y. D. Chong, and A. D. Stone, Phys. Rev. A **85**, 023802 (2012), arXiv: 1112.5167.
29 B. Peng, Ş. K. Özdemir, F. Lei, F. Monifi, M. Gianfreda, G. L. Long, S. Fan, F. Nori, C. M. Bender, and L. Yang, Nat. Phys. **10**, 394 (2014), arXiv: 1308.4564.
30 H. Jing, S. Özdemir, X. Y. Lü, J. Zhang, L. Yang, and F. Nori, Phys. Rev. Lett. **113**, 053604 (2014), arXiv: 1403.0657.
31 V. V. Konotop, J. Yang, and D. A. Zezyulin, Rev. Mod. Phys. **88**, 035002 (2016), arXiv: 1603.06826.
32 R. El-Ganainy, K. G. Makris, M. Khajavikhan, Z. H. Musslimani, S. Rotter, and D. N. Christodoulides, Nat. Phys. **14**, 11 (2018).
33 O. Sigwarth, and C. Miniatura, AAPPS Bull. **32**, 23 (2022).
34 C. Zheng, Europhys. Lett. **136**, 30002 (2021).
35 G. Q. Zhang, Z. Chen, D. Xu, N. Shammah, M. Liao, T. F. Li, L. Tong, S. Y. Zhu, F. Nori, and J. Q. You, PRX Quantum **2**, 020307 (2021), arXiv: 2104.09811.
36 X. Ni, D. Smirnova, A. Poddubny, D. Leykam, Y. Chong, and A. B. Khanikaev, Phys. Rev. B **98**, 165129 (2018).
37 D. X. Chen, Y. Zhang, J. L. Zhao, Q. C. Wu, Y. L. Fang, C. P. Yang, and F. Nori, Phys. Rev. A **106**, 022438 (2022), arXiv: 2209.02481.
38 H. Xu, D. G. Lai, Y. B. Qian, B. P. Hou, A. Miranowicz, and F. Nori, Phys. Rev. A **104**, 053518 (2021), arXiv: 2107.13891.
39 J. S. Tang, Y. T. Wang, S. Yu, D. Y. He, J. S. Xu, B. H. Liu, G. Chen, Y. N. Sun, K. Sun, Y. J. Han, C. F. Li, and G. C. Guo, Nat. Photon. **10**, 642 (2016).
40 Y. T. Wang, Z. P. Li, S. Yu, Z. J. Ke, W. Liu, Y. Meng, Y. Z. Yang, J. S. Tang, C. F. Li, and G. C. Guo, Phys. Rev. Lett. **124**, 230402 (2020).
41 J. Li, A. K. Harter, J. Liu, L. de Melo, Y. N. Joglekar, and L. Luo, Nat. Commun. **10**, 855 (2019).
42 H. Z. Chen, T. Liu, H. Y. Luan, R. J. Liu, X. Y. Wang, X. F. Zhu, Y. B. Li, Z. M. Gu, S. J. Liang, H. Gao, L. Lu, L. Ge, S. Zhang, J. Zhu, and R. M. Ma, Nat. Phys. **16**, 571 (2020).
43 C. Wu, A. Fan, and S. D. Liang, AAPPS Bull. **32**, 39 (2022).
44 C. Zheng, L. Hao, and G. L. Long, Phil. Trans. R. Soc. A. **371**, 20120053 (2013), arXiv: 1105.6157.
45 L. Xiao, K. Wang, X. Zhan, Z. Bian, K. Kawabata, M. Ueda, W. Yi, and P. Xue, Phys. Rev. Lett. **123**, 230401 (2019), arXiv: 1812.01213.
46 Y. Ashida, S. Furukawa, and M. Ueda, Nat. Commun. **8**, 15791 (2017), arXiv: 1611.00396.
47 H. Xu, D. Mason, L. Jiang, and J. G. E. Harris, Nature **537**, 80 (2016), arXiv: 1602.06881.
48 J. Doppler, A. A. Mailybaev, J. Böhm, U. Kuhl, A. Girschik, F. Libisch, T. J. Milburn, P. Rabl, N. Moiseyev, and S. Rotter, Nature **537**, 76 (2016).
49 K. Kawabata, Y. Ashida, and M. Ueda, Phys. Rev. Lett. **119**, 190401 (2017), arXiv: 1705.04628.
50 J. Wen, C. Zheng, Z. Ye, T. Xin, and G. Long, Phys. Rev. Res. **3**, 013256 (2021), arXiv: 2101.00175.
51 Y. L. Fang, J. L. Zhao, Y. Zhang, D. X. Chen, Q. C. Wu, Y. H. Zhou, C. P. Yang, and F. Nori, Commun. Phys. **4**, 223 (2021), arXiv: 2111.03803.
52 H. Shen, B. Zhen, and L. Fu, Phys. Rev. Lett. **120**, 146402 (2018), arXiv: 1706.07435.
53 K. Chen, and A. B. Khanikaev, Phys. Rev. B **105**, L081112 (2022), arXiv: 2111.12573.
54 Y. Choi, C. Hahn, J. W. Yoon, and S. H. Song, Nat. Commun. **9**, 2182 (2018).
55 D. C. Brody, J. Phys. A-Math. Theor. **47**, 035305 (2013), arXiv: 1308.2609.
56 F. K. Kunst, E. Edvardsson, J. C. Budich, and E. J. Bergholtz, Phys. Rev. Lett. **121**, 026808 (2018), arXiv: 1805.06492.
57 Q. C. Wu, Y. H. Chen, B. H. Huang, Y. Xia, and J. Song, Phys. Rev. A **94**, 053421 (2016), arXiv: 1604.04971.
58 C. Y. Ju, A. Miranowicz, G. Y. Chen, and F. Nori, Phys. Rev. A **100**, 062118 (2019), arXiv: 1906.08071.

59 K. Modi, A. K. Pati, A. Sen(De), and U. Sen, Phys. Rev. Lett. **120**, 230501 (2018).
60 Z. H. Liu, X. B. Liang, K. Sun, Q. Li, Y. Meng, M. Yang, B. Li, J. L. Chen, J. S. Xu, C. F. Li, and G. C. Guo, Phys. Rev. Lett. **126**, 170505 (2021), arXiv: 2011.04963.
61 C. Y. Ju, A. Miranowicz, F. Minganti, C. T. Chan, G. Y. Chen, and F. Nori, Phys. Rev. Res. **4**, 023070 (2022), arXiv: 2107.11910.
62 D. C. Brody, and E. M. Graefe, Phys. Rev. Lett. **109**, 230405 (2012), arXiv: 1208.5297.
63 L. Xiao, X. Zhan, Z. H. Bian, K. K. Wang, X. Zhang, X. P. Wang, J. Li, K. Mochizuki, D. Kim, N. Kawakami, W. Yi, H. Obuse, B. C. Sanders, and P. Xue, Nat. Phys. **13**, 1117 (2017).
64 D. F. V. James, P. G. Kwiat, W. J. Munro, and A. G. White, Phys. Rev. A **64**, 052312 (2001), arXiv: quant-ph/0103121.
65 M. Naghiloo, M. Abbasi, Y. N. Joglekar, and K. W. Murch, Nat. Phys. **15**, 1232 (2019), arXiv: 1901.07968.

Appendix

A1 Eigenstates of non-Hermitian Hamiltonians in biorthogonal quantum mechanics

We first briefly recall some important properties of non-Hermitian Hamiltonians in biorthogonal quantum mechanics [27, 28, 31, 32, 55-58]. Consider an arbitrary time-independent non-Hermitian Hamiltonian $\hat{H}$ with N eigenstates $\{|\phi_k\rangle\}$, $k = 1, 2, ..., N$. It satisfies the following eigenvalue equation:

$$\hat{H}|\phi_k\rangle = E_k|\phi_k\rangle. \tag{a1}$$

As the adjoint operator of $\hat{H}$, the Hamiltonian $\hat{H}^\dagger$ satisfies the following eigenvalue equation:

$$\hat{H}^\dagger|\widehat{\phi_k}\rangle = E_k^*|\widehat{\phi_k}\rangle, \tag{a2}$$

where $\{|\widehat{\phi_k}\rangle\}$ are the eigenstates of $\hat{H}^\dagger$ and also the biorthogonal partners of $\{|\phi_k\rangle\}$. The asterisk here means complex conjugate. The biorthogonal partners are normalized to satisfy the biorthogonality relation [55-58]

$$\langle\widehat{\phi_k}|\phi_l\rangle = \delta_{kl}, \tag{a3}$$

and the closure relation

$$\sum_k |\widehat{\phi_k}\rangle\langle\phi_k| = \sum_k |\phi_k\rangle\langle\widehat{\phi_k}| = 1. \tag{a4}$$

In this case, if the orthogonality of eigenstates in standard quantum mechanics is replaced by the biorthogonality that defines the relation between the quantum states in the Hilbert space and its dual space, the resulting quantum theory is called biorthogonal quantum mechanics [55-58]. Then, in biorthogonal quantum mechanics, the Hamiltonian $\hat{H}$ and its adjoint Hamiltonian $\hat{H}^\dagger$ can be expressed as:

$$\begin{aligned}\hat{H} &= \sum_k |\phi_k\rangle E_k\langle\widehat{\phi_k}|,\\ \hat{H}^\dagger &= \sum_k |\widehat{\phi_k}\rangle E_k^*\langle\phi_k|.\end{aligned} \tag{a5}$$

For simplicity, $\{\langle\widehat{\phi_k}|\}$ and $\{|\phi_k\rangle\}$ are called the left and right eigenstates of the Hamiltonian, respectively. In addition, the overlap distance Θ between two arbitrary pure states $|\psi\rangle = \sum_l c_l|\phi_l\rangle$ and $|\varphi\rangle = \sum_k d_k|\phi_k\rangle$ can be defined as [55]:

$$\cos^2\frac{\Theta}{2} = \frac{\langle\widehat{\psi}|\varphi\rangle\langle\widehat{\varphi}|\psi\rangle}{\langle\widehat{\psi}|\psi\rangle\langle\widehat{\varphi}|\varphi\rangle}, \tag{a6}$$

where $\langle\widehat{\psi}| = \sum_l c_l^*\langle\widehat{\phi_l}|$ and $\langle\widehat{\varphi}| = \sum_k d_k^*\langle\widehat{\phi_k}|$. In particular, $\Theta = 0$ only if $|\psi\rangle = \pm|\varphi\rangle$, whereas $\Theta = \pi$ only if $\langle\widehat{\varphi}|\psi\rangle = \langle\widehat{\psi}|\varphi\rangle = 0$. For a two-dimensional Hilbert space, the state $|\psi\rangle$ can be expressed in the form $|\psi\rangle = \cos\vartheta|\phi_1\rangle + \sin\vartheta e^{i\varphi}|\phi_2\rangle$, with $\langle\widehat{\psi}|\psi\rangle = 1$. The two eigenstates $|\phi_1\rangle$ and $|\phi_2\rangle$ here can be considered as antipodal points on the Bloch sphere. This is analogous to the counterpart of a Hermitian system, even though $|\phi_1\rangle$ and $|\phi_2\rangle$ may not be orthogonal, i.e., $\langle\phi_2|\phi_1\rangle \neq 0$. The usual Bloch sphere description is not adequate at the exceptional points (EPs). Since at the EPs the intended antipodal points ($|\phi_1\rangle$ and $|\phi_2\rangle$) completely overlap (i.e., $|\phi_1\rangle$=$|\phi_2\rangle$), the Bloch sphere will then become a dot naturally.

A2 Eigenstates and eigenvalues of non-Hermitian Hamiltonians in a $\mathcal{PT}$-symmetry single-qubit system

We start with a $\mathcal{PT}$-symmetry non-Hermitian Hamiltonian in a single-qubit system:

$$\hat{H}_{\mathcal{PT}} = s\hat{\sigma}_x + i\gamma\hat{\sigma}_z = \begin{pmatrix} i\gamma & s \\ s & -i\gamma \end{pmatrix}, \tag{a7}$$

where $s\hat{\sigma}_x$ is the Hermitian part of the Hamiltonian, $i\gamma\hat{\sigma}_z$ is the non-Hermitian part of the Hamiltonian governing gain or loss. Moreover, the parameter $s > 0$ is an energy scale, $a = \gamma/s > 0$ is a coefficient representing the degree of non-Hermiticity, and $\hat{\sigma}_x$ and $\hat{\sigma}_z$ are the standard Pauli operators. The eigenvalues and eigenvectors of $\hat{H}_{\mathcal{PT}}$ are given by

$$\begin{aligned}E_1 &= s\sqrt{1-a^2}, \quad |\phi_1\rangle = f_1 * (A_1|0\rangle + |1\rangle),\\ E_2 &= -s\sqrt{1-a^2}, \; |\phi_2\rangle = f_2 * (A_2|0\rangle + |1\rangle),\end{aligned} \tag{a8}$$

where $A_1 = ia + \sqrt{1-a^2}$, $A_2 = ia - \sqrt{1-a^2}$. Here, f_1 and f_2 are undetermined coefficients. The eigenvalues are real numbers for $0 < a < 1$ (the $\mathcal{PT}$-symmetry unbroken regime), while imaginary numbers for $a > 1$ (the $\mathcal{PT}$-symmetry broken regime). As the adjoint operator of $\hat{H}_{\mathcal{PT}}$, the eigenvalues and eigenvectors of $\hat{H}_{\mathcal{PT}}^\dagger$ are given by

$$\begin{aligned}E_1' &= s\sqrt{1-a^2}, \quad |\widehat{\phi_1}\rangle = f_3 * (-A_2|0\rangle + |1\rangle),\\ E_2' &= -s\sqrt{1-a^2}, \; |\widehat{\phi_2}\rangle = f_4 * (-A_1|0\rangle + |1\rangle),\end{aligned} \tag{a9}$$

where f_3 and f_4 are undetermined coefficients. By substituting eqs. (a8) and (a9) into eq. (a4), one can find that

$$f_1 \cdot f_3^* \times (1 - A_2^* A_1) = 1, \quad f_2 \cdot f_4^* \times (1 - A_1^* A_2) = 1. \tag{a10}$$

Theoretically, the coefficients f_1, f_2, f_3, and f_4 take arbitrary values provided they satisfy the relation (a10). However, the values of f_1, f_2, f_3, and f_4 may affect the transformation from the orthogonal space representation to the biorthogonal space representation.

In the $\mathcal{PT}$-symmetry unbroken regime, the dynamics of the non-Hermitian single-qubit system will gradually turn into the dynamics of a Hermitian single-qubit system when the parameter a (representing the degree of non-Hermiticity) tends to zero. In this case, one can set

$$\langle \phi_1 | \phi_1 \rangle = \langle \phi_2 | \phi_2 \rangle = 1, \tag{a11}$$

so that $|\phi_1\rangle$ and $|\phi_2\rangle$ are in line with basis states in the Hermitian single-qubit system. That is, $|f_1|^2 = 1 + |A_2|^2, |f_2|^2 = 1 + |A_1|^2$. Moreover, in the $\mathcal{PT}$-symmetry unbroken regime, by setting $\sin\theta = a$, one can find

$$\begin{aligned} &A_1 = \exp(\mathrm{i}\theta), \quad A_2 = -\exp(-\mathrm{i}\theta), \\ &\frac{1}{f_1 \cdot f_3^*} = \exp(2\mathrm{i}\theta) + 1, \quad \frac{1}{f_2 \cdot f_4^*} = \exp(-2\mathrm{i}\theta) + 1. \end{aligned} \tag{a12}$$

While, in the $\mathcal{PT}$-symmetry broken regime, by setting $\sin\theta = 1/a$, one has

$$A_1 = \mathrm{i}\cot\theta', \ A_2 = \mathrm{i}\tan\theta', \ f_1 \cdot f_3^* = f_2 \cdot f_4^* = 1/2. \tag{a13}$$

A3 Extended Noether's theorem for a $\mathcal{PT}$-symmetry system

Theoretically, there is more than one way to define the inner product in non-Hermitian systems. In biorthogonal quantum mechanics, the inner product for a non-Hermitian system is defined as [55-58]:

$$(\varphi, \psi) \equiv \langle \widehat{\varphi} | \psi \rangle = \sum_{k,l} d_k^* c_l \langle \widehat{\phi_k} | \phi_l \rangle = \sum_k d_k^* c_k, \tag{a14}$$

where $|\psi\rangle = \Sigma_l c_l |\phi_l\rangle$ ($|\varphi\rangle = \Sigma_k d_k |\phi_k\rangle$) is an arbitrary pure state with its associated state $\langle\widehat{\psi}| \equiv \Sigma_l c_l^* \langle\widehat{\phi_l}|$ ($\langle\widehat{\varphi}| \equiv \Sigma_k d_k^* \langle\widehat{\phi_k}|$).

Quantum systems are usually characterized by mixed states. Thus, it is significant to find the extension of Noether's theorem for mixed states. For a general $\mathcal{PT}$-symmetry system, its mixed state at any given time t can be expressed as a biorthogonal density operator:

$$\hat{\rho}_b(t) = \sum_{n=1}^{N} p_n |\psi_n(t)\rangle \langle \widehat{\psi_n(t)}|, \tag{a15}$$

where p_n is the probability of the system being in the pure state $|\psi_n(t)\rangle$, with $\langle\widehat{\psi_n}(t)|\psi_n(t)\rangle = 1$. Then, for the case of mixed states, the expectation value $(\hat{F})$ of an operator $\hat{F}$ is defined as [55]:

$$\begin{aligned} (\hat{F}) &\equiv \mathrm{tr}[\hat{\rho}_b(t)\hat{F}] \\ &= \sum_m \langle\widehat{\phi_m}|\hat{\rho}_b(t)\hat{F}|\phi_m\rangle \\ &= \sum_n \sum_m \langle\widehat{\phi_m}|p_n|\psi_n(t)\rangle\langle\widehat{\psi_n(t)}|\hat{F}|\phi_m\rangle \\ &= \sum_n p_n \sum_m \langle\widehat{\phi_m}|\psi_n(t)\rangle\langle\widehat{\psi_n(t)}|\hat{F}|\phi_m\rangle \\ &= \sum_n p_n \sum_m \langle\widehat{\psi_n(t)}|\hat{F}|\phi_m\rangle\langle\widehat{\phi_m}|\psi_n(t)\rangle \\ &= \sum_n p_n \langle\widehat{\psi_n(t)}|\hat{F}|\psi_n(t)\rangle, \end{aligned} \tag{a16}$$

where $\langle\widehat{\psi_n(t)}|\hat{F}|\psi_n(t)\rangle$ is the expectation value $(\hat{F})$ of the operator $\hat{F}$ for an arbitrary pure state $|\psi_n(t)\rangle$. Note that the closure relation $\sum_m |\phi_m\rangle\langle\widehat{\phi_m}| = 1$ has been applied to derive eq. (a16). Eq. (a16) is a natural generalization of the expectation value of an operator $\hat{F}$ for an arbitrary quantum state, either a mixed state or a pure state.

Furthermore, consider an arbitrary initial pure state $|\psi_n(0)\rangle = \Sigma_k c_k |\phi_k\rangle$ for a general $\mathcal{PT}$-symmetry system. According to the Schrödinger equation:

$$\frac{\mathrm{d}|\psi_n(t)\rangle}{\mathrm{d}t} = \frac{1}{\mathrm{i}\hbar}\hat{H}_{\mathcal{PT}}|\psi_n(t)\rangle, \tag{a17}$$

one can obtain the time-evolved state $|\psi_n(t)\rangle = \sum_k c_k \mathrm{e}^{-\mathrm{i}E_k t/\hbar}|\phi_k\rangle$ at any given time t and its associated state $\langle\widehat{\psi_n(t)}| = \sum_k c_k^* \mathrm{e}^{\mathrm{i}E_k^* t/\hbar}\langle\widehat{\phi_k}|$.

For a general $\mathcal{PT}$-symmetry system, the eigenvalues of the $\mathcal{PT}$-symmetry Hamiltonian $\hat{H}_{\mathcal{PT}}$ are real numbers in the $\mathcal{PT}$-symmetry unbroken regime. Whereas, the eigenvalues are complex numbers or purely imaginary numbers in the $\mathcal{PT}$-symmetry broken regime. Thus, in the $\mathcal{PT}$-symmetry unbroken regime, all the eigenvalues $\{E_k\}$ are real numbers (i.e., $E_k = E_k^*$), then $\langle\widehat{\psi_n(t)}|$ satisfies the following Schrödinger equation:

$$\begin{aligned} \frac{\mathrm{d}\langle\widehat{\psi_n(t)}|}{\mathrm{d}t} &= \frac{\mathrm{d}\sum_k c_k^* \mathrm{e}^{\mathrm{i}E_k^* t/\hbar}\langle\widehat{\phi_k}|}{\mathrm{d}t} \\ &= \sum_k \frac{\mathrm{i}E_k^*}{\hbar} c_k^* \mathrm{e}^{\mathrm{i}E_k^* t/\hbar}\langle\widehat{\phi_k}| \\ &= \sum_k \frac{\mathrm{i}E_k}{\hbar} c_k^* \mathrm{e}^{\mathrm{i}E_k^* t/\hbar}\langle\widehat{\phi_k}| \\ &= \sum_k \frac{\mathrm{i}}{\hbar} c_k^* \mathrm{e}^{\mathrm{i}E_k^* t/\hbar}[\hat{H}_{\mathcal{PT}}^\dagger|\widehat{\phi_k}\rangle]^\dagger \\ &= \frac{1}{-\mathrm{i}\hbar}\sum_k c_k^* \mathrm{e}^{\mathrm{i}E_k^* t/\hbar}\langle\widehat{\phi_k}|\hat{H}_{\mathcal{PT}} \end{aligned}$$

$$= \frac{1}{-\mathrm{i}\hbar}\langle\widehat{\psi_n(t)}|\hat{H}_{\mathcal{PT}}. \tag{a18}$$

Note that the relations $\hat{H}^{\dagger}|\widehat{\phi_k}\rangle = E_k^*|\widehat{\phi_k}\rangle$ and $[\hat{H}^{\dagger}_{\mathcal{PT}}|\widehat{\phi_k}\rangle]^{\dagger} = \langle\widehat{\phi_k}|\hat{H}_{\mathcal{PT}} = E_k\langle\widehat{\phi_k}|$ have been applied.

On the other hand, in the $\mathcal{PT}$-symmetry broken regime, all the eigenvalues $\{E_k\}$ are complex numbers or purely imaginary numbers. Without loss of generality, consider the eigenvalue E_k with a real part Re$[E_k]$ and a purely imaginary part Im$[E_k]$ (i.e., E_k=Re$[E_k]$+iIm$[E_k]$). Then $\langle\widehat{\psi_n(t)}|$ satisfies the following Schrödinger equation:

$$\begin{aligned}
&\frac{\mathrm{d}\langle\widehat{\psi_n(t)}|}{\mathrm{d}t}\\
&= \frac{\mathrm{d}\sum_k c_k^* \mathrm{e}^{\mathrm{i}E_k^* t/\hbar}\langle\widehat{\phi_k}|}{\mathrm{d}t}\\
&= \sum_k \frac{\mathrm{i}E_k^*}{\hbar} c_k^* \mathrm{e}^{\mathrm{i}E_k^* t/\hbar}\langle\widehat{\phi_k}|\\
&= \sum_k \frac{\mathrm{i}(-E_k + 2\mathrm{Re}[E_k])}{\hbar} c_k^* \mathrm{e}^{\mathrm{i}E_k^* t/\hbar}\langle\widehat{\phi_k}|\\
&= \frac{1}{\mathrm{i}\hbar}\sum_k c_k^* \mathrm{e}^{\mathrm{i}E_k^* t/\hbar}\langle\widehat{\phi_k}|(\hat{H}_{\mathcal{PT}} - 2\mathrm{Re}[E_k])\\
&= \frac{1}{\mathrm{i}\hbar}\langle\widehat{\psi_n(t)}|\hat{H}_{\mathcal{PT}} - \frac{1}{\mathrm{i}\hbar}\sum_k 2\mathrm{Re}[E_k] c_k^* \mathrm{e}^{\mathrm{i}E_k^* t/\hbar}\langle\widehat{\phi_k}|.
\end{aligned} \tag{a19}$$

Here we remark that provided $\hat{H}_{\mathcal{PT}}$ exhibits an exceptional point of the order of the matrix dimension [23, 65], then Re$[E_k]$=Re$[E_n]$, $\forall\ k$. Eq. (a19) can be reduced to

$$\frac{\mathrm{d}\langle\widehat{\psi_n(t)}|}{\mathrm{d}t} = \frac{1}{\mathrm{i}\hbar}\langle\widehat{\psi_n(t)}|(\hat{H}_{\mathcal{PT}} - 2\mathrm{Re}[E_n]). \tag{a20}$$

According to eq. (a16), the temporal evolution of the expectation value $(\hat{F})$ can be expressed as:

$$\begin{aligned}
&\frac{\mathrm{d}}{\mathrm{d}t}(\hat{F})\\
&= \sum_n p_n \frac{\mathrm{d}}{\mathrm{d}t}\langle\widehat{\psi_n(t)}|\hat{F}|\psi_n(t)\rangle\\
&= \sum_n p_n \left[\frac{\mathrm{d}\langle\widehat{\psi_n(t)}|}{\mathrm{d}t}|\hat{F}|\psi_n(t)\rangle\right.\\
&\quad \left.+\langle\widehat{\psi_n(t)}|\hat{F}|\frac{\mathrm{d}|\psi_n(t)\rangle}{\mathrm{d}t} + \langle\widehat{\psi_n(t)}|\frac{\mathrm{d}\hat{F}}{\mathrm{d}t}|\psi_n(t)\rangle\right].
\end{aligned} \tag{a21}$$

When the eigenvalues of the $\mathcal{PT}$-symmetry Hamiltonian $\hat{H}_{\mathcal{PT}}$ are real numbers, by substituting eqs. (a17) and (a18) into eq. (a21), one can find that the temporal evolution of the expectation value $(\hat{F})$ reads

$$\begin{aligned}
\frac{\mathrm{d}}{\mathrm{d}t}(\hat{F}) &= \sum_n p_n \left[\frac{1}{\mathrm{i}\hbar}(\hat{F}\hat{H}_{\mathcal{PT}} - \hat{H}_{\mathcal{PT}}\hat{F})_n + \left(\frac{\mathrm{d}\hat{F}}{\mathrm{d}t}\right)_n\right]\\
&= \sum_n p_n \left[\frac{1}{\mathrm{i}\hbar}([\hat{F}, \hat{H}_{\mathcal{PT}}])_n + \left(\frac{\mathrm{d}\hat{F}}{\mathrm{d}t}\right)_n\right]
\end{aligned} \tag{a22}$$

in the $\mathcal{PT}$-symmetry unbroken regime. Here, $(\cdot)_n = \langle\widehat{\psi_n(t)}|\cdot|\psi_n(t)\rangle$.

On the other hand, when the eigenvalues of the $\mathcal{PT}$-symmetry Hamiltonian $\hat{H}_{\mathcal{PT}}$ are imaginary numbers (Re$[E_k]$=0, $\forall\ k$), by substituting eqs. (a17) and (a20) into eq. (a21), one can find that the temporal evolution of the expectation value $(\hat{F})$ reads

$$\begin{aligned}
\frac{\mathrm{d}}{\mathrm{d}t}(\hat{F}) &= \sum_n p_n \left[\frac{1}{\mathrm{i}\hbar}(\hat{F}\hat{H}_{\mathcal{PT}} + \hat{H}_{\mathcal{PT}}\hat{F})_n + \left(\frac{\mathrm{d}\hat{F}}{\mathrm{d}t}\right)_n\right]\\
&= \sum_n p_n \left[\frac{1}{\mathrm{i}\hbar}(\{\hat{F}, \hat{H}_{\mathcal{PT}}\})_n + \left(\frac{\mathrm{d}\hat{F}}{\mathrm{d}t}\right)_n\right]
\end{aligned} \tag{a23}$$

in the $\mathcal{PT}$-symmetry broken regime. One can see that eq. (a22) is eq. (4) in the main text, while eq. (a23) is eq. (5) in the main text.

However, if the eigenvalues of the $\mathcal{PT}$-symmetry Hamiltonian $\hat{H}_{\mathcal{PT}}$ are not purely imaginary numbers (i.e., Re$[E_n] \neq 0$), then by substituting eqs. (a17) and (a20) into eq. (a21), one can find that the temporal evolution of the expectation value $(\hat{F})$ reads

$$\begin{aligned}
\frac{\mathrm{d}}{\mathrm{d}t}(\hat{F}) = \sum_n p_n &\left[\frac{1}{\mathrm{i}\hbar}(\hat{F}\hat{H}_{\mathcal{PT}} + \hat{H}_{\mathcal{PT}}\hat{F}\right.\\
&\left. -2\mathrm{Re}[E_n]\hat{F})_n + \left(\frac{\mathrm{d}\hat{F}}{\mathrm{d}t}\right)_n\right]
\end{aligned} \tag{a24}$$

in the $\mathcal{PT}$-symmetry broken regime. In this case, even if $\hat{H}_{\mathcal{PT}}$ and $\hat{F}$ satisfy the anti-commutation relation $\{\hat{H}_{\mathcal{PT}}, \hat{F}\} = 0$, the expectation value $(\hat{F})$ is not a constant of motion.

Therefore, in order to obtain a conserved expectation value $(\hat{F})$ and connect the chiral symmetry with the conserved operator in the $\mathcal{PT}$-symmetry broken regime, for the $\mathcal{PT}$-symmetry systems considered in this work, the eigenvalues of $\hat{H}_{\mathcal{PT}}$ should change from real numbers to purely imaginary numbers. We note that such $\mathcal{PT}$-symmetric systems have been widely used to investigate the dynamics of non-Hermitian systems in the presence of balanced gain and loss [24,26,39,45,49-51,62,63]. In these cases, the extended Noether's theorem presented in our work applies well.

A4 Conditions for obtaining real expectation values in a $\mathcal{PT}$-symmetry system

From an experimental point of view, it is preferable to keep expectation values as real numbers. In the following, we will briefly explore some conditions for obtaining real expectation values in a $\mathcal{PT}$-symmetry system.

In standard quantum mechanics, consider an N-dimensional Hilbert space:

$$\mathscr{H}_S = \mathrm{Span}\{|\phi_1^{'}\rangle, |\phi_2^{'}\rangle, ..., |\phi_N^{'}\rangle\}, \tag{a25}$$

where the basis state $|\phi_k^{'}\rangle$ ($k = 1, 2, ..., N$), satisfies the orthogonality relation

$$\langle\phi_k^{'}|\phi_l^{'}\rangle = \delta_{kl}, \tag{a26}$$

and the closure relation

$$\sum_{k=1}^{N} |\phi_k^{'}\rangle\langle\phi_k^{'}| = 1. \tag{a27}$$

Note that the basis state $|\phi_k^{'}\rangle$ here is not the eigenstate of the $\mathcal{PT}$-symmetry Hamiltonian.

A time-independent operator $\hat{F}$ can be expressed by a density operator:

$$\hat{F} = \sum_{k,l} F_{kl}|\phi_k^{'}\rangle\langle\phi_l^{'}|, \tag{a28}$$

where $F_{kl} = \langle\phi_k^{'}|\hat{F}|\phi_l^{'}\rangle$ is the density matrix element of the operator $\hat{F}$. Suppose that the time-evolved state of the $\mathcal{PT}$-symmetry system reads $|\psi_n(t)\rangle = \sum_k D_k(t)|\phi_k^{'}\rangle$ at any given time t and its associated state is $\langle\psi_n(t)| = \sum_k D_k^*(t)\langle\phi_k^{'}|$. Here, $D_k(t)$ is a time-dependent and undetermined coefficient. Then, the standard expectation value $\langle\hat{F}\rangle$ for the pure state $|\psi_n(t)\rangle$ reads

$$\begin{aligned}\langle\hat{F}\rangle &= \langle\psi_n(t)|\hat{F}|\psi_n(t)\rangle \\ &= \sum_i D_i^*(t)\langle\phi_i^{'}| \sum_{k,l} F_{kl}|\phi_k^{'}\rangle\langle\phi_l^{'}| \sum_j D_j(t)|\phi_j^{'}\rangle \\ &= \sum_{k,l} D_k^*(t)F_{kl}D_l(t) \\ &= \sum_k |D_k(t)|^2 F_{kk} + \sum_{k\neq l} D_k^*(t)D_l(t)F_{kl}.\end{aligned} \tag{a29}$$

If the time-independent operator $\hat{F}$ is Hermitian in the N-dimensional Hilbert space:

$$\hat{F} = \sum_{k,l} F_{kl}|\phi_k^{'}\rangle\langle\phi_l^{'}| = \hat{F}^\dagger = \sum_{k,l} F_{lk}^*|\phi_k^{'}\rangle\langle\phi_l^{'}|, \tag{a30}$$

one can obtain that F_{kk} should be a real number and $F_{kl} = F_{lk}^*$ ($k \neq l$). In this case, the standard expectation value $\langle\hat{F}\rangle$ (see eq. (a29)) must be a real number, because $|D_k(t)|^2 F_{kk}$ is real and

$$\begin{aligned}&\sum_{k\neq l} D_k^*(t)D_l(t)F_{kl} \\ &= \sum_{k\neq l,k<l} \left[D_k^*(t)D_l(t)F_{kl} + D_l^*(t)D_k(t)F_{lk}\right] \\ &= \sum_{k\neq l,k<l} \left[D_k^*(t)D_l(t)F_{kl} + (D_k^*(t)D_l(t)F_{kl})^*\right] \\ &= \sum_{k\neq l,k<l} 2\mathrm{Re}[D_k^*(t)D_l(t)F_{kl}],\end{aligned} \tag{a31}$$

where the relation $F_{lk} = F_{kl}^*$ ($k \neq l$) has been applied. Thus, the condition for obtaining a real standard expectation value $\langle\hat{F}\rangle$ in a $\mathcal{PT}$-symmetry system is that the chosen operator $\hat{F}$ is Hermitian in standard quantum mechanics.

In a similar way, one can prove that the condition for obtaining a real biorthogonal expectation value $(\hat{F})$ in a $\mathcal{PT}$-symmetry system is that the chosen operator $\hat{F}$ is Hermitian in biorthogonal quantum mechanics. Here, we note that in biorthogonal quantum mechanics, the biorthogonality relation and the closure relation (see eqs. (a3) and (a4)) are applied. A time-independent operator $\hat{F}$ can be expressed by a biorthogonal density operator:

$$\hat{F} = \sum_{k,l} F_{kl}|\phi_k\rangle\langle\widehat{\phi_l}|, \tag{a32}$$

where $F_{kl} = \langle\phi_k|\hat{F}|\widehat{\phi_l}\rangle$ is the biorthogonal density matrix element of the operator $\hat{F}$. Moreover, according to eq. (a16), the biorthogonal expectation value $(\hat{F})$ reads

$$\begin{aligned}(\hat{F}) &= \sum_n p_n\langle\widehat{\psi_n(t)}|\hat{F}|\psi_n(t)\rangle \\ &= \sum_n p_n \sum_i C_i^*(t)\langle\widehat{\phi_i}| \sum_{k,l} F_{kl}|\phi_k\rangle\langle\widehat{\phi_l}| \sum_j C_j(t)|\phi_j\rangle \\ &= \sum_n p_n \sum_{k,l} C_k^*(t)F_{kl}C_l(t) \\ &= \sum_n p_n \left[\sum_k |C_k(t)|^2 F_{kk} + \sum_{k\neq l} C_k^*(t)C_l(t)F_{kl}\right],\end{aligned} \tag{a33}$$

where the time-evolved state $|\psi_n(t)\rangle = \sum_k C_k(t)|\phi_k\rangle$ and its associated state $\langle\widehat{\psi_n(t)}| = \sum_k C_k^*(t)\langle\widehat{\phi_k}|$ with $C_k(t) = c_k\mathrm{e}^{-\mathrm{i}E_k t/\hbar}$ can be obtained from eq. (a17).

If the time-independent operator $\hat{F}$ is Hermitian in the biorthogonal Hilbert space:

$$\hat{F} = \sum_{k,l} F_{kl}|\phi_k\rangle\langle\widehat{\phi_l}| = \hat{F}^\dagger = \sum_{k,l} F_{lk}^*|\phi_k\rangle\langle\widehat{\phi_l}|, \tag{a34}$$

one can obtain that F_{kk} is a real number and also $F_{kl} = F_{lk}^*$ ($k \neq l$). Then, the biorthogonal expectation value $(\hat{F})$ (see eq. (a33)) must be a real number, because p_n and $|C_k(t)|^2 F_{kk}$ are real and

$$\begin{aligned}&\sum_{k\neq l} C_k^*(t)C_l(t)F_{kl} \\ &= \sum_{k\neq l,k<l} \left[C_k^*(t)C_l(t)F_{kl} + C_l^*(t)C_k(t)F_{lk}\right] \\ &= \sum_{k\neq l,k<l} \left[C_k^*(t)C_l(t)F_{kl} + (C_k^*(t)C_l(t)F_{kl})^*\right] \\ &= \sum_{k\neq l,k<l} 2\mathrm{Re}[C_k^*(t)C_l(t)F_{kl}],\end{aligned} \tag{a35}$$

where the relation $F_{lk} = F_{kl}^*$ ($k \neq l$) has been applied. That is, the condition for obtaining a real biorthogonal expectation value $(\hat{F})$ in a $\mathcal{PT}$-symmetry system is that the chosen operator $\hat{F}$ is Hermitian in biorthogonal quantum mechanics.

Therefore, in the main text, in order to ensure that the chosen operators $\hat{F}$ in eqs. (7) and (8) are Hermitian in biorthogonal quantum mechanics, the coefficients c_1 and c_2 in eq. (7) are real numbers, and the coefficient $\tilde{c}_1$ in eq. (8) is a purely imaginary number. In addition, when we experimentally investigate the "biorthogonal" expectation value $(\hat{F})$, the two deformed Pauli operators $\widetilde{\sigma}_z$ and $\widetilde{\sigma}_y$ (which are Hermitian in biorthogonal quantum mechanics) are applied. When we experimentally investigate the standard expectation value $\langle \hat{F} \rangle$, the two standard Pauli operators $\hat{\sigma}_z$ and $\hat{\sigma}_y$ (which are Hermitian in standard quantum mechanics) are chosen.

A5 Decomposition of the nonunitary time-evolution operator

The dynamic evolution of a $\mathcal{PT}$-symmetry single-qubit system is characterized by the nonunitary time-evolution operator $U_{\mathcal{PT}} = \exp(-\mathrm{i}\hat{H}_{\mathcal{PT}})$, with the $\mathcal{PT}$-symmetry Hamiltonian $\hat{H}_{\mathcal{PT}} = s(\hat{\sigma}_x + \mathrm{i}a\hat{\sigma}_z)$. Without loss of generality, we set $s = 1$. In our experiment, we implement the nonunitary time-evolution operator $U_{\mathcal{PT}}$ by decomposing it into basic operators.

Let us start with

$$\begin{aligned}\hat{U}_{\mathcal{PT}}(t) &= \exp(-\mathrm{i}\hat{H}_{\mathcal{PT}}t)\\ &= \exp\left[-\mathrm{i}(\sigma_x + \mathrm{i}a\sigma_z)t\right]\\ &= \exp\left[\begin{pmatrix} a & -\mathrm{i} \\ -\mathrm{i} & -a \end{pmatrix} t\right]\\ &= \begin{pmatrix} A+B & -\mathrm{i}C \\ -\mathrm{i}C & A-B \end{pmatrix}.\end{aligned} \tag{a36}$$

Here A, B and C are given by

(1) for $0 < a < 1$,

$$A = \cos(\omega t),\quad B = \frac{a}{\omega}\sin(\omega t),\quad C = \frac{1}{\omega}\sin(\omega t), \tag{a37}$$

where $\omega = \sqrt{1-a^2} > 0$.

(2) for $a \geq 1$,

$$A = \cosh(\omega t),\quad B = \frac{a}{\omega}\sinh(\omega t),\quad C = \frac{1}{\omega}\sinh(\omega t), \tag{a38}$$

where $\omega = \sqrt{a^2-1} \geq 0$.

We set the parameters

$$A = \frac{1}{2}(\lambda_2 + \lambda_1)\sin(-2\theta_1 + \theta_2 - \pi/4), \tag{a39}$$

$$B = \frac{1}{2}(\lambda_2 - \lambda_1)\sin(2\theta_1 + \theta_2 - \pi/4), \tag{a40}$$

$$\begin{aligned}C = &-[\lambda_2 \sin 2\theta_1 \cos(\theta_2 + \pi/4)\\ &+ \lambda_1 \cos 2\theta_1 \sin(\theta_2 + \pi/4)],\end{aligned} \tag{a41}$$

$$\theta_2 = \left(2k_1 + \frac{3}{4}\right)\pi - 2\theta_1, \tag{a42}$$

$$\theta_3 = \left(\frac{k_2}{2} + \frac{1}{8}\right)\pi - \theta_1, \tag{a43}$$

where k_1 and k_2 are integers. Base on eqs. (a39)-(a43), the parameters $\lambda_1, \lambda_2, \theta_1, \theta_2$, and θ_3 can be determined with given A, B, and C. The matrix eq. (a36) can thus be decomposed as follows:

$$\begin{aligned}\hat{U}_{\mathcal{PT}}(t) = &\begin{pmatrix} U_{11} & U_{12} \\ U_{21} & U_{22} \end{pmatrix}\begin{pmatrix} 0 & \lambda_1 \\ \lambda_2 & 0 \end{pmatrix}\begin{pmatrix} 1 & 0 \\ 0 & -1 \end{pmatrix}\\ &\times\begin{pmatrix} \cos 2\theta_1 & \sin 2\theta_1 \\ \sin 2\theta_1 & -\cos 2\theta_1 \end{pmatrix}\begin{pmatrix} 1 & 0 \\ 0 & \mathrm{i} \end{pmatrix},\end{aligned} \tag{a44}$$

where

$$U_{11} = \frac{\mathrm{i}}{\sqrt{2}}\mathrm{e}^{-\mathrm{i}\pi/4}(\sin\theta_2 + \cos\theta_2)\,\mathrm{e}^{\mathrm{i}(\theta_2 - 2\theta_3)}, \tag{a45}$$

$$U_{12} = \frac{\mathrm{i}}{\sqrt{2}}\mathrm{e}^{-\mathrm{i}\pi/4}(\sin\theta_2 - \cos\theta_2)\,\mathrm{e}^{\mathrm{i}(\theta_2 - 2\theta_3)}, \tag{a46}$$

$$U_{21} = \frac{1}{\sqrt{2}}\mathrm{e}^{-\mathrm{i}\pi/4}(\sin\theta_2 - \cos\theta_2)\,\mathrm{e}^{-\mathrm{i}(\theta_2 - 2\theta_3)}, \tag{a47}$$

$$U_{22} = \frac{1}{\sqrt{2}}\mathrm{e}^{-\mathrm{i}\pi/4}(\sin\theta_2 + \cos\theta_2)\,\mathrm{e}^{-\mathrm{i}(\theta_2 - 2\theta_3)}. \tag{a48}$$

A half-wave plate (HWP) and a quarter-wave plate (QWP) realize rotation operations, which are described by the following operators:

$$\hat{R}_{\mathrm{QWP}}(\alpha) = \begin{pmatrix} \cos^2\alpha + \mathrm{i}\sin^2\alpha & (\sin 2\alpha\cos\alpha)/2 \\ (\sin 2\alpha\cos\alpha)/2 & \sin^2\alpha + \mathrm{i}\cos^2\alpha \end{pmatrix}, \tag{a49}$$

$$\hat{R}_{\mathrm{HWP}}(\beta) = \begin{pmatrix} \cos 2\beta & \sin 2\beta \\ \sin 2\beta & -\cos 2\beta \end{pmatrix}, \tag{a50}$$

where α and β are tunable setting angles. Based on eqs. (a49) and (a50), we have

$$\begin{aligned}&\hat{R}_{\mathrm{QWP}}(45^\circ)\hat{R}_{\mathrm{HWP}}(\theta_3)\hat{R}_{\mathrm{QWP}}(\theta_2)\\ &= \begin{pmatrix} 1+\mathrm{i} & 1-\mathrm{i} \\ 1-\mathrm{i} & 1+\mathrm{i} \end{pmatrix}\begin{pmatrix} \cos 2\theta_3 & \sin 2\theta_3 \\ \sin 2\theta_3 & -\cos 2\theta_3 \end{pmatrix}\\ &\times\begin{pmatrix} \cos^2\theta_2 + \mathrm{i}\sin^2\theta_2 & \sin\theta_2\cdot\cos\theta_2(1-\mathrm{i}) \\ \sin\theta_2\cdot\cos\theta_2(1-\mathrm{i}) & \sin^2\theta_2 + \mathrm{i}\cos^2\theta_2 \end{pmatrix}\\ &= \begin{pmatrix} U_{11} & U_{12} \\ U_{21} & U_{22} \end{pmatrix},\end{aligned} \tag{a51}$$

$$\hat{R}_{\mathrm{HWP}}(0^\circ) = \begin{pmatrix} 1 & 0 \\ 0 & -1 \end{pmatrix}, \tag{a52}$$

$$\hat{R}_{\mathrm{QWP}}(0^\circ) = \begin{pmatrix} 1 & 0 \\ 0 & \mathrm{i} \end{pmatrix}, \tag{a53}$$

$$\hat{R}_{\rm HWP}(\theta_3)=\begin{pmatrix}\cos 2\theta_3 & \sin 2\theta_3\\ \sin 2\theta_3 & -\cos 2\theta_3\end{pmatrix}. \tag{a54}$$

After inserting eqs. (a51)-(a54) into eq. (a44), we obtain

$$\begin{aligned}\hat{U}_{\mathcal{PT}}=&\hat{R}_{\rm QWP}(\pi/4)\hat{R}_{\rm HWP}(\theta_3)\hat{R}_{\rm QWP}(\theta_2)\hat{M}(\xi_1,\ \xi_2)\\ &\hat{R}_{\rm HWP}(0)\hat{R}_{\rm HWP}(\theta_1)\hat{R}_{\rm QWP}(0),\end{aligned} \tag{a55}$$

with

$$\hat{M}=\begin{pmatrix}0 & \lambda_1\\ \lambda_2 & 0\end{pmatrix}. \tag{a56}$$

The matrix $\hat{M}$ can be expressed as:

$$\hat{M}=c\begin{pmatrix}0 & \sin 2\xi_1\\ \sin 2\xi_2 & 0\end{pmatrix}, \tag{a57}$$

where $c=\lambda_1/\sin 2\xi_1=\lambda_2/\sin 2\xi_2$ is a trivial constant. For simplicity, we define

$$\hat{L}(\xi_1,\xi_2)=\begin{pmatrix}0 & \sin 2\xi_1\\ \sin 2\xi_2 & 0\end{pmatrix}. \tag{a58}$$

Thus, we have $\hat{M}=c\hat{L}$. Note that the functions of both operators $\hat{L}$ and $c\hat{L}$ are identical. This is because the states $\hat{L}|\psi\rangle$ and $c\hat{L}|\psi\rangle$, obtained by enforcing the two operators $\hat{L}$ and $c\hat{L}$ on an arbitrary state $|\psi\rangle$, are the same according to the principles of quantum mechanics. Therefore, we can replace $\hat{M}$ in eq. (a55) by the operator $\hat{L}$. In this sense, we have from eq. (a55):

$$\begin{aligned}\hat{U}_{\mathcal{PT}}=&\hat{R}_{\rm QWP}(\pi/4)\hat{R}_{\rm HWP}(\theta_3)\hat{R}_{\rm QWP}(\theta_2)\hat{L}(\xi_1,\ \xi_2)\\ &\times\hat{R}_{\rm HWP}(0)\hat{R}_{\rm HWP}(\theta_1)\hat{R}_{\rm QWP}(0),\end{aligned} \tag{a59}$$

which is exactly the same as the decomposition of the nonunitary time-evolution operator $\hat{U}_{\mathcal{PT}}$, described by eq. (9) in the main text.

A6 Reverse extraction of quantum information in biorthogonal quantum mechanics

Although the mathematical expressions of a given quantum state are different in standard quantum mechanics and biorthogonal quantum mechanics, the physical meaning of the given quantum state must be the same. Based on this idea, for a given quantum state, one can obtain a one-to-one corresponding relation between the density matrix in standard quantum mechanics and the density matrix in biorthogonal quantum mechanics.

For instance, in the orthogonal representation for standard quantum mechanics, a quantum state at any given time t can be given by a density operator:

$$\hat{\rho}(t)=\sum_{n,m}\rho_{nm}(t)|n\rangle\langle m|=\sum_{n}\lambda_n|\varphi_n(t)\rangle\langle\varphi_n(t)|. \tag{a60}$$

Note that $\{\rho_{nm}(t)\}$ are the density matrix elements of the density operator $\hat{\rho}(t)$ at any given time t in standard quantum mechanics, which can be experimentally obtained via quantum state tomography. Then, based on the obtained density matrix elements $\{\rho_{nm}(t)\}$, one can calculate the eigenvalues $\{\lambda_n\}$ and eigenstates $\{|\varphi_n(t)\rangle\}$ of the density operator $\hat{\rho}(t)$.

On the other hand, according to biorthogonal quantum mechanics, the density operator $\hat{\rho}_b(t)$ of a quantum state at any given time t in biorthogonal representation can be expressed as:

$$\hat{\rho}_b(t)=\sum_{n}\lambda_n|\varphi_n(t)\rangle\langle\widehat{\varphi_n(t)}|=\sum_{n,m}\widetilde{\rho}_{nm}(t)|\phi_n\rangle\langle\widehat{\phi_m}|, \tag{a61}$$

where $\widetilde{\rho}_{nm}(t)=\langle\widehat{\phi_m}|\hat{\rho}_b(t)|\phi_n\rangle$ carries the key quantum information of a quantum state in biorthogonal quantum mechanics. Note that the eigenvalues $\{\lambda_n\}$ and the eigenstates $\{|\varphi_n(t)\rangle\}$ can be obtained from eq. (a60), while $\{\langle\widehat{\phi_m}|\}$ and $\{|\phi_n\rangle\}$ are the left and right eigenstates of the non-Hermitian Hamiltonian of the system, and they can be obtained from eqs. (a1) and (a2). In this way, we can reversely extract the exact information $\widetilde{\rho}_{nm}(t)$ (in biorthogonal quantum mechanics) of a given quantum state from its density operator in standard quantum mechanics.

A7 Dynamical evolution of a class of $\mathcal{PT}$-symmetry systems in biorthogonal quantum mechanics

Note that the dynamical evolution of a class of $\mathcal{PT}$-symmetry systems in biorthogonal quantum mechanics is quite different from that in standard quantum mechanics. In biorthogonal quantum mechanics, a mixed state $\hat{\rho}_b(t)$ at any given time t can be expressed as a biorthogonal density operator:

$$\hat{\rho}_b(t)=\sum_{n}p_n\hat{\rho}_{b,n}(t)=\sum_{n}p_n|\psi_n(t)\rangle\langle\widehat{\psi_n(t)}|, \tag{a62}$$

where p_n is the probability of the system being in the pure state $|\psi_n(t)\rangle$, and $\hat{\rho}_{b,n}(t)=|\psi_n(t)\rangle\langle\widehat{\psi_n(t)}|$.

Let us first consider the system to be in the pure state $|\psi_n(t)\rangle$. When the eigenvalues of the $\mathcal{PT}$-symmetry Hamiltonian $\hat{H}_{\mathcal{PT}}$ are real numbers, the system works in the $\mathcal{PT}$-symmetry unbroken regime. In this case, according to eqs. (a17) and (a18), one can obtain the temporal evolution of the density operator $\hat{\rho}_{b,n}(t)$,

$$\begin{aligned}&\frac{{\rm d}\hat{\rho}_{b,n}(t)}{{\rm d}t}\\ &=\frac{{\rm d}|\psi_n(t)\rangle\langle\widehat{\psi_n(t)}|}{{\rm d}t}\\ &=\left(\frac{H_{\mathcal{PT}}}{{\rm i}\hbar}|\psi_n(t)\rangle\langle\widehat{\psi_n(t)}|+|\psi_n(t)\rangle\langle\widehat{\psi_n(t)}|\frac{-H_{\mathcal{PT}}}{{\rm i}\hbar}\right)\end{aligned}$$

$$= \frac{1}{\mathrm{i}\hbar}[H_{\mathcal{PT}}\hat{\rho}_{b,n}(t) - \hat{\rho}_{b,n}(t)H_{\mathcal{PT}}]. \tag{a63}$$

On the other hand, when the eigenvalues of the $\mathcal{PT}$-symmetry Hamiltonian $\hat{H}_{\mathcal{PT}}$ are imaginary numbers, the system works in the $\mathcal{PT}$-symmetry broken regime. In this situation, according to eqs. (a17) and (a19), one can find that the temporal evolution of the density operator $\hat{\rho}_{b,n}(t)$ follows:

$$\begin{aligned}&\frac{\mathrm{d}\hat{\rho}_{b,n}(t)}{\mathrm{d}t}\\&= \frac{\mathrm{d}|\psi_n(t)\rangle\langle\widehat{\psi_n(t)}|}{\mathrm{d}t}\\&= \frac{H_{\mathcal{PT}}}{\mathrm{i}\hbar}|\psi_n(t)\rangle\langle\widehat{\psi_n(t)}| + |\psi_n(t)\rangle\langle\widehat{\psi_n(t)}|\frac{H_{\mathcal{PT}}}{\mathrm{i}\hbar}\\&= \frac{1}{\mathrm{i}\hbar}[H_{\mathcal{PT}}\hat{\rho}_{b,n}(t) + \hat{\rho}_{b,n}(t)H_{\mathcal{PT}}].\end{aligned} \tag{a64}$$

Moreover, one can verify that $\hat{\rho}_{b,n}(t) = U_{\mathcal{PT}}(t)\hat{\rho}_{b,n}(0)U'_{\mathcal{PT}}(t)$ satisfies the following relation:

$$\begin{aligned}&\frac{\mathrm{d}\hat{\rho}_{b,n}(t)}{\mathrm{d}t}\\&= \frac{\mathrm{d}U_{\mathcal{PT}}(t)}{\mathrm{d}t}\hat{\rho}_{b,n}(0)U'_{\mathcal{PT}}(t) + U_{\mathcal{PT}}(t)\hat{\rho}_{b,n}(0)\frac{\mathrm{d}U'_{\mathcal{PT}}(t)}{\mathrm{d}t}\\&= \frac{1}{\mathrm{i}\hbar}[H_{\mathcal{PT}}\hat{\rho}_{b,n}(t) - \hat{\rho}_{b,n}(t)H_{\mathcal{PT}}],\end{aligned} \tag{a65}$$

where $\hat{U}_{\mathcal{PT}}(t)$=exp$(-\mathrm{i}\hat{H}_{\mathcal{PT}}t/\hbar)$ and $\hat{U}'_{\mathcal{PT}}(t)$=exp$(\mathrm{i}\hat{H}_{\mathcal{PT}}t/\hbar)$ are time-evolution operators. Then, comparing eq. (a63) with eq. (a65), one can see that $\hat{\rho}_{b,n}(t) = U_{\mathcal{PT}}(t)\hat{\rho}_{b,n}(0)U'_{\mathcal{PT}}(t)$ is the general solution of eq. (a63) in the $\mathcal{PT}$-symmetry unbroken regime. Similarly, it is easy to prove that $\hat{\rho}_{b,n}(t) = U_{\mathcal{PT}}(t)\hat{\rho}_{b,n}(0)U_{\mathcal{PT}}(t)$ satisfies the following relation:

$$\begin{aligned}&\frac{\mathrm{d}\hat{\rho}_{b,n}(t)}{\mathrm{d}t}\\&= \frac{\mathrm{d}U_{\mathcal{PT}}(t)}{\mathrm{d}t}\hat{\rho}_{b,n}(0)U_{\mathcal{PT}}(t) + U_{\mathcal{PT}}(t)\hat{\rho}_{b,n}(0)\frac{\mathrm{d}U_{\mathcal{PT}}(t)}{\mathrm{d}t}\\&= \frac{1}{\mathrm{i}\hbar}[H_{\mathcal{PT}}\hat{\rho}_{b,n}(t) + \hat{\rho}_{b,n}(t)H_{\mathcal{PT}}].\end{aligned} \tag{a66}$$

One then has that $\hat{\rho}_{b,n}(t) = U_{\mathcal{PT}}(t)\hat{\rho}_{b,n}(0)U_{\mathcal{PT}}(t)$ is the general solution of eq. (a64) in the $\mathcal{PT}$-symmetry broken regime by comparing eq. (a64) with eq. (a66).

Let us now consider the system to be in the mixed state $\hat{\rho}_b(t)$. After substituting $\hat{\rho}_{b,n}(t) = U_{\mathcal{PT}}(t)\hat{\rho}_{b,n}(0)U'_{\mathcal{PT}}(t)$ and $\hat{\rho}_{b,n}(t) = U_{\mathcal{PT}}(t)\hat{\rho}_{b,n}(0)U_{\mathcal{PT}}(t)$ into eq. (a62), it is then straightforward that the temporal evolution of the density operator $\hat{\rho}_b(t)$ follows:

$$\hat{\rho}_b(t) = \hat{U}_{\mathcal{PT}}(t)\hat{\rho}_b(0)\hat{U}'_{\mathcal{PT}}(t), \tag{a67}$$

$$\hat{\rho}_b(t) = \hat{U}_{\mathcal{PT}}(t)\hat{\rho}_b(0)\hat{U}_{\mathcal{PT}}(t), \tag{a68}$$

where eq. (a67) corresponds to the case when the system works in the $\mathcal{PT}$-symmetry unbroken regime, while eq. (a68) corresponds to the case when the system works in the $\mathcal{PT}$-symmetry broken regime. One can see that eq. (a67) is eq. (12) in the main text, while eq. (a68) is eq. (13) in the main text.